7448.2-E

U. S. ARMY RESEARCH OFFICE - DURHAM
CONTRACT NO. DAHC04-69-C-0019

70-11

AD705378

STRESS CONCENTRATION IN AN ELASTOMERIC SHEET SUBJECT TO LARGE DEFORMATIONS

by

Alexander Segal and Jerome M. Klosner

This document has been approved for public release and sale; its distribution is unlimited.

POLYTECHNIC INSTITUTE OF BROOKLYN

DEPARTMENT
of
AEROSPACE ENGINEERING
and
APPLIED MECHANICS

MARCH 1970

DDC
RECEIVED
MAY 11 1970
C

DISTRIBUTION OF THIS DOCUMENT IS UNLIMITED

Reproduced by the CLEARINGHOUSE for Federal Scientific & Technical Information Springfield Va. 22151

PIBAL REPORT No. 70-11

DISCLAIMER NOTICE

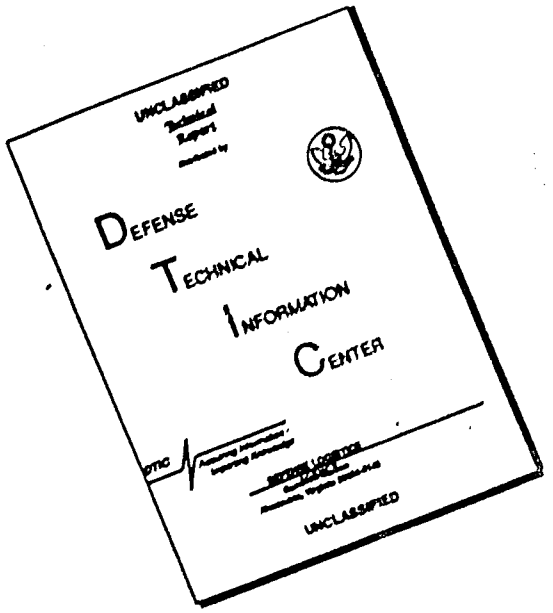

THIS DOCUMENT IS BEST QUALITY AVAILABLE. THE COPY FURNISHED TO DTIC CONTAINED A SIGNIFICANT NUMBER OF PAGES WHICH DO NOT REPRODUCE LEGIBLY.

U. S. Army Research Office - Durham
Contract No. DAHC04-69-C-0019

STRESS CONCENTRATION IN AN ELASTOMERIC SHEET SUBJECT TO LARGE DEFORMATIONS

by

Alexander Segal and Jerome M. Klosner

Polytechnic Institute of Brooklyn

Department of

Aerospace Engineering and Applied Mechanics

March 1970

PIBAL Report No. 70-11

Reproduction in whole or in part is permitted for any purpose of the United States Government. Distribution of this document is unlimited.

ABSTRACT

Biaxial and uniaxial experiments have been conducted on a thin sheet of natural rubber, which can be assumed to be incompressible, isotropic, and perfectly elastic. The strain energy function and constitutive equations have been determined, and the material is classified as a Generalized Rivlin-Mooney type.

Biaxial experiments were then conducted on the same sheet with a circular cutout and stress concentration factors were obtained. Results indicate a significant increase in the factor with increased displacements.

A modified Particle - In - Cell (P.I.C.) method has been developed and analytical results were obtained for a sheet with a rigid circular inclusion. It is shown that the stress concentration factor for a Rivlin-Mooney material increases with increasing deformations, a result which is in qualitative agreement with solutions obtained by other methods [31,32]. The use of the Generalized Rivlin-Mooney material, however, leads to a decrease in stress concentration with increasing deformations.

LIST OF SYMBOLS

$a^{\alpha\beta}, A^{\alpha\beta}$	contravarient components of in-plane metric tensors of undeformed and deformed body
C_1, C_2	Rivlin-Mooney material constants
g^{ij}, G^{ij}	contravarient components of metric tenors of undeformed and deformed body
I_1, I_2, I_3	strain invariants
K_r	stress concentration factor at boundary of rigid inclusion (ratio of radial stress at boundary of inclusion to that at edge of sheet)
K_t	stress concentration factor at hole boundary (ratio of tangential stress at edge of hole to that at edge of sheet)
k	cell spacing used in M.I.C. method
$n_{\alpha\beta}$	stress resultant
q_α	shear resultant
r_o	radius of undeformed hole
u,v	displacement components
u_1, v_1	displacements at edge of sheet
W	strain energy density function (per unit volume of undeformed body)
X,Y,Z	coordinates of a point in deformed body
X_1, Y_1	coordinates of sides of deformed sheet
x,y,z	coordinates of a point in undeformed body

x_1, y_1	coordinates of sides of undeformed sheet
τ_{ij}	physical component of stress tensor
λ_∞	ratio of deformed to undeformed length of membrane
λ_x (or λ_1), λ_y (or λ_2)	elongation ratios in x (or 1) and y (or 2) directions respectively
$(\lambda_x)_\infty$, $(\lambda_y)_\infty$	ratio of deformed to undeformed lengths in x and y directions respectively
σ_{ij}	component of stress tensor

I. INTRODUCTION

An ever increasing use of reinforced and unreinforced polymeric materials in complex technological situations has given impetus to the general study of elastomeric materials subject to large deformations[1-10]. But, owing to the nonlinearities of the basic equations for such materials, analytical solutions have been obtained for only a limited number of problems. In general the material is assumed to be perfectly elastic and incompressible, and the deformations are homogeneous or highly symmetric, so that nonlinear partial differential equations can be avoided in the analysis (see, for example, Chapter III of Ref. 7 for discussion of the work of Rivlin, also see Refs. 6, 11-18).

Although the literature dealing with the classical stress concentration problem for linear elastic materials abounds, (see for example Refs. 19-22) only very few investigations can be found which realistically treat the stress concentration of elastomeric materials subject to large deformations. The reason lies in the difficulty in solving the nonlinear partial differential equations which govern the stress and displacement fields.

One way of attacking such problems is to use the method of successive approximation to obtain solutions[1,10,23-25]. In such cases the stress and displacement fields are expanded into power series in a characteristic real parameter ε, which depends on the nature of

the problem. When these series expansions are substituted into the field equations of finite elasticity, the coefficients of the successive powers of ε in the resulting identities yield linear equations for the determination of the successive terms in the power series expansions. The parameter ε is so chosen that the identities corresponding to the first degree in ε coincide with the set of field equations in the classical linear theory. Because of the lengthy calculations required most of the problems actually solved in this manner have been limited to the first and the second degree in ε. In particular, Adkins et al[26-28] applied this method to plane problems, and, by using the complex variable technique[19], obtained second-order solutions for an infinite plate with a circular hole or a circular rigid inclusion, subjected to a uniaxial tension at infinity. The results showed that for a Mooney material the degree of stress concentration at the hole is reduced as the load is increased. Similar observations were made by Guz', Savin and Tsurpal[29] in their study of an infinite plate of physically nonlinear material having a circular hole. They assumed that the displacement field was within the range of applicability of infinitesimal strain theory. In a recent paper, Evans and Pister[30] investigated the same problem by using a power series expansion up to the third order. They showed that unless the deviation from linearity in the stress-strain relation is very small, the series solutions do not converge rapidly enough to lead to reasonable approximations to the exact solutions.

Another way of solving the resulting nonlinear equations of the stress concentration problem is to employ numerical procedures. Using a forward integration method, Rivlin and Thomas[31] solved the problem of the axially symmetric deformation produced in a circular sheet of a Mooney material, containing a central circular hole, when subjected to radial tensile forces at its outer periphery. Their displacement results were found to be in good agreement with the experimental measurements on a test piece of vulcanized natural rubber. No results on stress concentration was presented. Recently, Yang[32] re-investigated the axisymmetric problem and was able to reduce the equations to two decoupled first-order equations, which were solved numerically by the Runge-Kutta method. The results, for both the hole and the rigid inclusion, indicate that the stress and strain concentration factors increase with increasing load for the Mooney material. An analysis of the displacements obtained by Rivlin and Thomas[31] reveals the same trend for the concentration factors.

In this thesis, the problem of a highly elastic sheet with a centered circular hole or rigid circular inclusion, subjected to a general biaxial stress state, is considered. Since we consider very large deformations and general biaxial stress states, none of the previous approaches are applicable. Instead the nonlinear partial differential equations are linearized by adopting an incremental procedure. A variation of the Particle-In-Cell (P.I.C.) method, which has been so successfully applied to hydrodynamic blast problems[33-36], is developed specifically for

this type of elliptic problem. Essentially, the method combines the features of the Eulerian and Lagrangian approaches by introducing an Eulerian computational mesh and by keeping track of the material particles as in a Lagrangian formulation. A description of this method can be found in Chapter II, Section H.

Two series of experiments have been conducted. One, was carried out on the sheet without the hole, in order to characterize the mechanical properties of the rubber for use in the analytical calculations. The second set were the biaxial stress concentration experiments performed on the sheet with the hole.

2. THEORY

A. Equilibrium Equations for a Thin Plane Sheet[7,10]

Consider a flat elastic sheet whose thickness before deformation h_o is constant and is small compared to its other dimensions. The sheet undergoes a finite deformation symmetrical about the middle plane $z = 0$ which thus becomes the middle plane $Z = 0$ in the deformed state. X, Y, Z are the coordinates of a point in the deformed body which before deformation was at x,y,z, where both sets of coordinates are referred to the same rectangular cartesian system.

The equilibrium equations, in the absence of body and inertia forces, are:

$$-^{ij}\|_i = 0 \qquad (2\text{-}1)$$

where the double line denotes covariant differentiation with respect to i(X,Y, or Z). Since in rectangular coordinates the components of the stress tensor τ^{ij} coincide with the physical components of the stress σ_{ij}, Eq. (2-1) can be written as:

$$\sigma_{ij},_i = 0 \qquad (2\text{-}2)$$

where σ_{ij} is the stress per unit area of the deformed body.

Integrating the equilibrium equations (2-2), and noting that the surfaces of the plate are traction free, we obtain

$$n_{\alpha\beta,\alpha} = 0 \quad (\alpha,\beta = X,Y) \tag{2-3}$$

where

$$n_{\alpha\beta} = \int_{-h}^{h} \sigma_{\alpha\beta}\, dZ \tag{2-4}$$

is the stress resultant per unit length of the deformed plate and h is its thickness. The shear resultant

$$q_{\alpha} = \int_{-h}^{h} \sigma_{\alpha Z}\, dZ = 0 \tag{2-5}$$

due to the symmetrical stress distribution about the middle plane.

We define a scalar function λ which represents the extension ratio at the middle plane $Z = 0$ in a direction normal to it,

$$\lambda = \frac{\partial Z}{\partial z} \qquad (Z = 0) \tag{2-6}$$

Thus

$$\lim_{h_o \to 0} \frac{h}{h_o} = \lim_{Z \to 0} \frac{\partial Z}{\partial z} = \lambda \tag{2-7}$$

From (2-4):

$$\frac{n_{\alpha\beta}}{2h_o} = \frac{1}{2h_o}\int_{-h}^{h} \sigma_{\alpha\beta}\, dZ \qquad (2\text{-}8)$$

and from (2-7)

$$\lim_{h_o \to 0} \frac{n_{\alpha\beta}}{2h_o} = \lambda(\sigma_{\alpha\beta})_{Z=0}$$

Since the faces of the sheet are free from applied forces

$$\lim_{h_o \to 0} [\sigma_{ZZ}]_{Z=0} = 0 \qquad (2\text{-}9)$$

For very small h_o we can approximately write

$$[\sigma_{ZZ}]_{Z=0} = 0$$

and
$$n_{\alpha\beta} = 2h_o\, \lambda(\sigma_{\alpha\beta})_{Z=0} \qquad (2\text{-}10)$$

Substituting (2-10) into (2-3), we obtain the final form of the membrane equilibrium equations

$$(\lambda\sigma_{\alpha\beta})_{,\alpha} = 0 \quad (Z=0) \qquad (2\text{-}11)$$

or

$$\frac{\partial}{\partial X}(\lambda\sigma_{XX}) + \frac{\partial}{\partial Y}(\lambda\sigma_{XY}) = 0 \quad (Z = 0)$$

$$\frac{\partial}{\partial X}(\lambda\sigma_{XY}) + \frac{\partial}{\partial Y}(\lambda\sigma_{YY}) = 0 \quad (Z = 0) \qquad (2\text{-}12)$$

B. Constitutive Equations

If the sheet is made of a homogeneous, isotropic, elastic and incompressible material

$$I_3 = 1 \qquad (2\text{-}13)$$

and the strain energy density function W (measured per unit volume of the undeformed body) takes the form

$$W = W(I_1, I_2) \qquad (2\text{-}14)$$

The inplane stresses on the middle plane can then be written as[10]

$$\tau_{\alpha\beta} = \sigma_{\alpha\beta} = H\, a^{\alpha\beta} + L\, A^{\alpha\beta} \quad (\alpha,\beta = X,Y) \qquad (2\text{-}15)$$

where

$$H = 2\left(\frac{\partial W}{\partial I_1} + \lambda^2 \frac{\partial W}{\partial I_2}\right)$$

$$L = -2\lambda^2 \frac{\partial W}{\partial I_1} - 2(\lambda^2 I_1 - \lambda^4 - 1/\lambda^2) \frac{\partial W}{\partial I_2} \qquad (2\text{-}16)$$

and $a^{\alpha\beta}$, $A^{\alpha\beta}$ are the inp'ane components at $Z = 0$ of the metric tensors (g^{ij}) of the undeformed and (G^{ij}) deformed body, respectively. Thus the general metric tensors at $Z = 0$ are written as:

$$[G_{ij}]_{Z=0} = \begin{bmatrix} A_{11} & A_{12} & G_{13} \\ A_{12} & A_{22} & G_{23} \\ G_{13} & G_{23} & G_{33} \end{bmatrix} \quad ; \quad [g_{ij}]_{Z=0} = \begin{bmatrix} a_{11} & a_{12} & g_{13} \\ a_{12} & a_{22} & g_{23} \\ g_{13} & g_{23} & g_{33} \end{bmatrix} \tag{2-17}$$

where

$$G_{ij} = \frac{\partial y^r}{\partial \theta^i} \frac{\partial y^r}{\partial \theta^j} \quad ; \quad g_{ij} = \frac{\partial x^r}{\partial \theta^i} \frac{\partial x^r}{\partial \theta^j}$$

$$(i,j = 1,2,3 \; ; \; y^r = X,Y,Z \; ; \; x^r = x,y,z) \tag{2-18}$$

and θ_i are general curvilinear coordinates. We shall choose θ_i so that they coincide with the rectangular cartesian coordinates, X, Y, Z. Thus we see that

$$G_{ij} = \delta_{ij} \quad ; \quad A_{\alpha\beta} = \delta_{\alpha\beta}$$

and

$$G^{ij} = \delta^{ij} \quad ; \quad A^{\alpha\beta} = \delta^{\alpha\beta} \tag{2-19}$$

Hence

$$A = |A_{\alpha\beta}| = |G_{ij}| = 1$$

Since the deformation has been assumed to be symmetrical about the middle plane it follows that x and y are even functions of Z, and thus at Z = 0 we have

$$x = x(X,Y) \qquad y = y(X,Y)$$

$$\frac{\partial x}{\partial Z} = \frac{\partial y}{\partial Z} = 0 \quad , \quad \frac{\partial z}{\partial X} = \frac{\partial z}{\partial Y} = 0 \tag{2-20}$$

$$\frac{\partial Z}{\partial x} = \frac{\partial Z}{\partial y} = 0 \quad , \quad \frac{\partial X}{\partial z} = \frac{\partial Y}{\partial z} = 0$$

and $$\frac{\partial Z}{\partial z} = \lambda \qquad \frac{\partial z}{\partial Z} = 1/\lambda \tag{2-21}$$

where $\lambda = \lambda(X,Y)$ represents the extension ratio at the middle plane in the Z direction and is assumed to be finite and nonzero. We now can substitute Eqs. (2-20) and (2-21) into (2-17) and (2-18) to obtain the values of the components of the metric tensors g_{ij}, g^{ij} at the plane $Z = 0$.

$$g_{XX} = a_{XX} = \left(\frac{\partial x}{\partial X}\right)^2 + \left(\frac{\partial y}{\partial X}\right)^2$$

$$g_{XY} = a_{XY} = \frac{\partial x}{\partial X}\frac{\partial x}{\partial Y} + \frac{\partial y}{\partial X}\frac{\partial y}{\partial Y}$$

$$g_{YY} = a_{YY} = \left(\frac{\partial x}{\partial Y}\right)^2 + \left(\frac{\partial y}{\partial Y}\right)^2$$

$$g_{ZZ} = \left(\frac{\partial z}{\partial Z}\right)^2 = 1/\lambda^2$$

$$g_{XZ} = g_{YZ} = 0 \tag{2-22}$$

or $$g_{ij} = \begin{bmatrix} a_{XX} & a_{XY} & 0 \\ a_{XY} & a_{YY} & 0 \\ 0 & 0 & 1/\lambda^2 \end{bmatrix} \tag{2-23}$$

and $$g = |g_{ij}| = a/\lambda^2 \tag{2-24}$$

where $$a = |a_{\alpha\beta}| = a_{XX}\, a_{YY} - (a_{XY})^2 \tag{2-25}$$

The component of the contravariant metric tensors g^{ij} and $a^{\alpha\beta}$ can be determined from the equation:

$$g^{ij} = \frac{\text{cofactor } g_{ij}}{g} \tag{2-26}$$

and are therefore

$$g^{XX} = a^{XX} = \frac{a_{YY}/\lambda^2}{a/\lambda^2} = \frac{a_{YY}}{a}$$

$$g^{XY} = a^{XY} = -\frac{a_{XY}/\lambda^2}{a/\lambda^2} = -\frac{a_{XY}}{a}$$

$$g^{YY} = a^{YY} = \frac{a_{XX}/\lambda^2}{a/\lambda^2} = \frac{a_{XX}}{a}$$

$$g^{ZZ} = \frac{a}{a/\lambda^2} = \lambda^2 \tag{2-27}$$

$$g^{XZ} = g^{YZ} = 0$$

or
$$g^{ij} = \begin{bmatrix} a^{XX} & a^{XY} & 0 \\ a^{XY} & a^{YY} & 0 \\ 0 & 0 & \lambda^2 \end{bmatrix} \tag{2-28}$$

and
$$|g^{ij}| = \lambda^2 \left[a^{XY}\, a^{YY} - (a^{XY})^2\right] = \frac{\lambda^2}{a} \tag{2-29}$$

The strain invariants are given by the expressions

$$I_1 = g^{rs} G_{rs} = \lambda^2 + a^{rs} A_{rs}$$

$$I_2 = g_{rs} G^{rs} \tau_3 = \frac{1}{\lambda^2} + a_{rs} A^{rs} \qquad (2\text{-}30)$$

$$\tau_3 = G/g = \frac{\lambda^2 A}{a} = 1$$

and therefore $a = \lambda^2$ because of incompressibility.

Finally, then $$I_1 = \frac{a_{XX} + a_{YY} + a^2}{a}$$

$$\tau_2 = a_{XX} + a_{YY} + 1/a \qquad (2\text{-}31)$$

The most general power series form of W for an incompressible homogeneous isotropic elastic material is[37]

$$W = \sum_{i=0}^{\infty} \sum_{j=0}^{\infty} C_{ij} (\tau_1 - 3)^i (I_2 - 3)^j \qquad (2\text{-}32)$$

where C_{ij} are constants and $C_{oo} = 0$.

In the following, we assume a Rivlin-Mooney type of material which is expressed by

$$W = C_1 (I_1 - 3) + C_2 (I_2 - 3) \qquad (2\text{-}33)$$

The necessary and sufficient conditions for $W \geq 0$ is that $C_1 \geq 0$ and $C_2 \geq 0$. Substitution of (2-31) and (2-33) into (2-16) yields

$$H = 2(C_1 + a\,C_2)$$

$$L = -\,2a\,C_1 - 2(a_{XX} + a_{YY} - 1/a)C_2 \qquad (2\text{-}34)$$

Finally, the stresses of Eq. (2-15) can be written as follows:

$$\sigma_{XX} = 2C_1\,\frac{a_{YY}}{a} - 2C_2\,a_{XX} - 2aC_1 + 2\,\frac{C_2}{a}$$

$$\sigma_{YY} = 2C_1\,\frac{a_{XX}}{a} - 2C_2\,a_{YY} - 2aC_1 + 2\,\frac{C_2}{a} \qquad (2\text{-}35)$$

$$\sigma_{XY} = -\,2(C_1 + aC_2)\,\frac{a_{XY}}{a}$$

C. Displacement Equilibrium Equations

Replacing X and Y by the indices 1 and 2, respectively, and appealing to Eqs. (2-35), we have

$$\lambda\sigma_{XX} = \lambda\sigma_{11} = 2\,\frac{C_1}{\sqrt{a}}\,a_{22} - 2C_2\sqrt{a}\,a_{11} - 2\sqrt{a^3}C_1 + 2\,\frac{C_2}{\sqrt{a}}$$

$$\lambda\sigma_{YY} = \lambda\sigma_{22} = 2\,\frac{C_1\,a_{11}}{\sqrt{a}} - 2C_2\sqrt{a}\,a_{22} - 2\sqrt{a^3}C_1 + 2\,\frac{C_2}{\sqrt{a}} \qquad (2\text{-}36)$$

$$\lambda\sigma_{XY} = \lambda\sigma_{12} = -\,2(C_1 + aC_2)\,\frac{a_{12}}{\sqrt{a}}$$

The equilibrium equations (2-12) then may be expressed as

$$C[2a(a_{12,2} - a_{22,1}) + (a_{22} + 3a^2)\,a_{,1} - a_{12}\,a_{,2}]$$

$$+ a_{,1} + a(a_{11}a_{,1} + a_{12}\,a_{,2}) + 2a^2(a_{12,2} + a_{11,1}) = 0 \qquad (2\text{-}37)$$

and $$C[2a(a_{12,1} - a_{11,2}) + (a_{11} + 3a^2)\, a_{,2} - a_{12}\, a_{,1}]$$
$$+ a_{,2} + a(a_{22}\, a_{,2} + a_{12}\, a_{,1}) + 2a^2(a_{12,1} + a_{22,2}) = 0 \qquad (2\text{-}38)$$

where $$C = C_1/C_2 \quad , \qquad (2\text{-}39)$$

and a comma denotes partial differentiation with respect to 1 or 2 (X or Y).

We define the displacements in terms of the coordinates of the deformed body

$$u(X,Y) = X - x(X,Y)$$
$$v(X,Y) = Y - y(X,Y) \qquad (2\text{-}40)$$

Thus in terms of these displacements

$$a_{11} = (1-u_{,1})^2 + (v_{,1})^2$$
$$a_{22} = (u_{,2})^2 + (1-v_{,2})^2 \qquad (2\text{-}41)$$
$$a_{12} = -[(1-u_{,1})u_{,2} + (1-v_{,2})v_{,1}]$$
$$a = [(1-u_{,1})(1-v_{,2}) - u_{,2}\, v_{,1}]^2$$

and the equilibrium equations in terms of the displacements are

$$C[(\gamma_1^2+v_{,1}^2)(u_{,22}\gamma_2+v_{,22}u_{,2}) + 2(\gamma_1 u_{,2}+\gamma_2 v_{,1})(u_{,12}\gamma_2+v_{,12}u_{,2})$$
$$+ (\gamma_2^2+u_{,2}^2)(u_{,11}\gamma_2+v_{,11}u_{,2}) + 3(\gamma_1\gamma_2-u_{,2}v_{,1})^4(u_{,11}\gamma_2+v_{,12}\gamma_1+u_{,21}v_{,1}+u_{,2}v_{,11})]$$
$$+ (u_{,11}\gamma_2+v_{,21}\gamma_1+u_{,21}v_{,1}+u_{,2}v_{,11}) - (\gamma_1\gamma_2-u_{,2}v_{,1})^2[u_{,11}(-v_{,1}^2\gamma_2-3\gamma_1^2\gamma_2+2u_{,2}v_{,1}\gamma_1)$$
$$+ u_{,12}(-\gamma_1^2 v_{,1}-v_{,1}^3+2u_{,2}\gamma_1\gamma_2+v_{,1}\gamma_2^2-u_{,2}^2 v_{,1}) + u_{,22}(2u_{,2}v_{,1}\gamma_1-\gamma_1^2\gamma_2+v_{,1}^2\gamma_2)$$
$$+ v_{,11}(-\gamma_1^2 u_{,2}+2v_{,1}\gamma_1\gamma_2-3u_{,2}v_{,1}^2) + v_{,12}(-\gamma_1^3-v_{,1}^2\gamma_1+u_{,2}^2\gamma_1+2u_{,2}v_{,1}\gamma_2-\gamma_1\gamma_2^2)$$
$$+ v_{,22}(u_{,2}\gamma_1^2+2v_{,1}\gamma_1\gamma_2-u_{,2}v_{,1}^2)] = 0 \qquad (2\text{-}42a)$$

and

$$C[(\gamma_2^2+u_{,2}^2)(v_{,11}\gamma_1+u_{,11}v_{,1}) + 2(\gamma_2 v_{,1}+\gamma_1 u_{,2})(v_{,12}\gamma_1+u_{,12}v_{,1})$$
$$+ (\gamma_1^2+v_{,1}^2)(v_{,22}\gamma_1+u_{,22}v_{,1}) + 3(\gamma_2\gamma_1-v_{,1}u_{,2})^4(\gamma_1 v_{,22}+\gamma_2 u_{,12}+v_{,12}u_{,2}+v_{,1}u_{,22})]$$
$$+ (v_{,22}\gamma_1+u_{,12}\gamma_2+v_{,12}u_{,2}+v_{,1}u_{,22}) - (\gamma_2\gamma_1-v_{,1}u_{,2})^2[v_{,22}(-u_{,2}^2\gamma_1-3\gamma_1\gamma_2^2+2v_{,1}u_{,2}\gamma_2)$$
$$+ v_{,12}(-u_{,2}\gamma_2^2-u_{,2}^3+2v_{,1}\gamma_1\gamma_2+u_{,2}\gamma_1^2-u_{,2}v_{,1}^2) + v_{,11}(2u_{,2}v_{,1}\gamma_2-\gamma_1\gamma_2^2+u_{,2}^2\gamma_1)$$
$$+ u_{,22}(-\gamma_2^2 v_{,1}+2u_{,2}\gamma_1\gamma_2-3u_{,2}^2 v_{,1}) + u_{,12}(-\gamma_2^3-u_{,2}^2\gamma_2+v_{,1}^2\gamma_2+2u_{,2}v_{,1}\gamma_1-\gamma_1^2\gamma_2)$$
$$+ u_{,11}(v_{,1}\gamma_2^2+2u_{,2}\gamma_1\gamma_2-u_{,2}^2 v_{,1})] = 0 \qquad (2\text{-}42b)$$

where $\gamma_1 = 1 - u_{,1}$, $\gamma_2 = 1 - v_{,2}$ (2-43)

D. Piecewise Linearization of the Equilibrium Equations

The two equilibrium equations (2-42) are second order nonlinear partial differential equations in u and v. In order to solve for u and v we assume that the body is strained to its final position by

successive steps of small displacement increments Δu and Δv. The total displacement after n+1 such steps is expressed as

$$u^{n+1} = \sum_{i=1}^{n} \Delta u^i + \Delta u^{n+1} = u^n + \Delta u^{n+1}$$
$$v^{n+1} = \sum_{i=1}^{n} \Delta v^i + \Delta v^{n+1} = v^n + \Delta v^{n+1} \qquad (2\text{-}44)$$

where $$u^n = \sum_{i=1}^{n} \Delta u^i \quad , \quad v^n = \sum_{i=1}^{n} \Delta v^i \qquad (2\text{-}45)$$

It is assumed that Δu, Δv are sufficiently small so that terms containing squares or higher order terms in Δu, Δv or their partial derivatives can be neglected with respect to first order terms. Thus, for example,

$$(1-u_{,1}^{n+1})^2 = (1-u_{,1}^{n}-\Delta u_{,1}^{n+1})^2 = (1-u_{,1}^{n})^2 - 2(1-u_{,1}^{n})\Delta u_{,1}^{n+1} + 0(\Delta u_{,1}^{n+1})^2 \qquad (2\text{-}46)$$

Following this assumption all the expressions appearing in the equilibrium equations are rewritten by expressing u, v in the forms of (2-44) and retaining only first order terms in Δu, Δv and their derivatives. For simplicity, the superscripts of u^n, v^n, Δu^{n+1}, Δv^{n+1} will be omitted in writing the following linearized form of the equilibrium equations at the $(n+1)^{th}$ step

$$A_{11}\,\Delta u_{,11} + A_{22}\,\Delta u_{,22} + A_{12}\,\Delta u_{,12} + A_1\,\Delta u_{,1} + A_2\,\Delta u_{,2}$$
$$+ B_{11}\,\Delta v_{,11} + B_{22}\,\Delta v_{,22} + B_{12}\,\Delta v_{,12} + B_1\,\Delta v_{,1} + B_2\,\Delta v_{,2} + K_1 = 0 \qquad (2\text{-}47a)$$

and

$$D_{11}\,\Delta u_{,11} + D_{22}\,\Delta u_{,22} + D_{12}\,\Delta u_{,12} + D_1\,\Delta u_{,1} + D_2\,\Delta u_{,2}$$
$$+ E_{11}\,\Delta v_{,11} + E_{22}\,\Delta v_{,22} + E_{12}\,\Delta v_{,12} + E_1\,\Delta v_{,1} + E_2\,\Delta v_{,2} + K_2 = 0 \qquad (2\text{-}47b)$$

The coefficients A_{11}, ..., B_{11}, ..., K_1, D_{11}, ..., E_{11}, ..., K_2 are to be found in Appendix A and are functions of the derivatives of the total displacements at the completion of the n^{th} step and contain the Rivlin-Mooney constants.

E. Modified P.I.C. Method

The linearized equilibrium equations (2-47) are solved numerically by using a modified form of the P.I.C. Method, which has been successfully used in wave propagation problems[34]. The procedure follows.

First a fixed grid (Eulerian) is introduced, dividing the region into a finite number of cells. The displacement of each cell is represented by the displacement at its center. The partial derivatives of Δu, Δv are expressed in finite difference form at each of the cell centers, which act as the pivotal points. The substitution of these finite difference forms into the differential equations (2-47), produces a set of linear algebraic equations in the set of unknowns, Δu and Δv, at each point. The incremental displacements determined in this first

(Eulerian) part satisfy the equilibrium equations in the sense of classical linear theory, where it is assumed that the final coordinates are identical with the initial ones. The geometric nonlinear effect, due to changes in the configuration of the material, is accounted for in the second part of the procedure.

We begin by distributing particles in each cell, where a cell (i,j) is the square around mesh point (i,j) bounded by the lines $i \pm k/2$ and $j \pm k/2$. These particles move during each step, and their incremental displacements are assumed to be the same as that of the cell center in which they find themselves at the beginning of a step. The position and total displacements of these particles are recorded throughout the deformation. In solving for the incremental displacements of the $n+1^{th}$ step, for example, it is necessary to know at each cell center the total displacements accumulated during the first n steps. These displacements are assumed to be equal to the average displacements of all the particles in the cell at the end of the n^{th} step. If no particles move in or out of a cell then its displacement remains unmodified.

At the end of each load step the nonlinear equations are checked so as to be sure that the assumption of piecewise linearity is reasonable. If the check fails, the step has to be refined and the computation repeated.

F. Extension of a Thin Elastic Sheet with a Hole at its Center

Consider a rectangular sheet subjected to biaxial extensions along its sides. The sheet contains a traction free hole at its center.

The method of solution described can be applied to a hole of arbitrary shape. If the hole is symmetrical with respect to the axes of symmetry of the sheet, then it is sufficient to consider only one quarter of the sheet. In what follows, a hole with such symmetry is assumed, and the analysis is thus carried out for only one quarter of the sheet. The surface of the sheet is divided into cells by introducing a grid system (Fig. 1). The pivotal points are located at the cell centers and have a constant spacing k. The partial derivatives at i,j, expressed in central difference form are:

$$
\begin{aligned}
u,_1(i,j) &= [u(i+k,j) - u(i-k,j)]/2k + 0(k^2) \\
u,_2(i,j) &= [u(i,j+k) - u(i,j-k)]/2k + 0(k^2) \\
u,_{11}(i,j) &= [u(i+k,j) - 2u(i,j) + u(i-k,j)]/k^2 + 0(k^2) \\
u,_{22}(i,j) &= [u(i,j+k) - 2u(i,j) + u(i,j-k)]/k^2 + 0(k^2) \\
u,_{12}(i,j) &= [u(i+k,j+k) - u(i-k,j+k) - u(i+k,j-k) + u(i-k,j-k)]/4k^2 + 0(k^2)
\end{aligned}
\qquad (2\text{-}48)
$$

Introducing such forms for the partial derivatives into the equilibrium equations (2-47) results in a set of algebraic equations with each equation containing the unknowns Δu, Δv of point (i,j) and the eight surrounding points. Thus the equilibrium equations in central difference form are

$$
\begin{aligned}
&A_{12}\,\Delta u(i-k,j-k) + (4A_{22}-2kA_2)\,\Delta u(i,j-k) - A_{12}\Delta u(i+k,j-k) + (4A_{11}-2kA_1)\Delta u(i-k,j) \\
&- 8(A_{11}+A_{22})\,\Delta u(i,j) + (4A_{11}+2kA_1)\,\Delta u(i+k,j) - A_{12}\Delta u(i-k,j+k) \\
&+ (4A_{22}+2kA_2)\,\Delta u(i,j+k) + A_{12}\,\Delta u(i+k,j+k) + B_{12}\,\Delta v(i-k,j-k)
\end{aligned}
$$

(continued on next page)

$$+ (4B_{22}-2kB_2)\,\Delta v(i,j-k) - B_{12}\,\Delta v(i+k,j-k) + (4B_{11}-2kB_1)\,\Delta v(i-k,j)$$
$$- 8(B_{11}+B_{22})\,\Delta v(i,j) + (4B_{11}+2kB_1)\,\Delta v(i+k,j) - B_{12}\,\Delta v(i-k,j+k)$$
$$+ (4B_{22}+2kB_2)\,\Delta v(i,j+k) + B_{12}\,\Delta v(i+k,j+k) + K_1 = 0 \qquad (2\text{-}49a)$$

and

$$D_{12}\,\Delta u(i-k,j-k) + (4D_{22}-2kD_2)\,\Delta u(i,j-k) - D_{12}\,\Delta u(i+k,j-k)$$
$$+ (4D_{11}-2kD_1)\,\Delta u(i-k,j) - 8(D_{11}+D_{22})\,\Delta u(i,j) + (4D_{11}+2kD_1)\,\Delta u(i+k,j)$$
$$- D_{12}\,\Delta u(i-k,j+k) + (4D_{22}+2kD_2)\,\Delta u(i,j+k) + D_{12}\,\Delta u(i+k,j+k) + E_{12}\,\Delta v(i-k,j-k)$$
$$+ (4E_{22}-2kE_2)\,\Delta v(i,j-k) - E_{12}\,\Delta v(i+k,j-k) + (4E_{11}-2kE_1)\,\Delta v(i-k,j)$$
$$- 8(E_{11}+E_{22})\,\Delta v(i,j) + (4E_{11}+2kE_1)\,\Delta v(i+k,j) - E_{12}\,\Delta v(i-k,j+k)$$
$$+ (4E_{22}+2kE_2)\,\Delta v(i,j+k) + E_{12}\,\Delta v(i+k,j+k) + K_2 = 0 \qquad (2\text{-}49b)$$

Boundary Conditions

The x - and y - axes are axes of symmetry, and, consequently,

$$u(1,j) = 0 \qquad \text{on the y-axis,}$$

and
$$u(1-k,j) = -\,u(1+k,j)\;;\quad v(1-k,j) = v(1+k,j), \qquad (2\text{-}50)$$

while
$$v(i,1) = 0 \qquad \text{on the x-axis,}$$

and
$$u(i,1-k) = u(i,1+k)\;;\quad v(i,1-k) = -\,v(i,1+k) \qquad (2\text{-}51)$$

Let $x = x_1$ and $y = y_1$ be the sides of the undeformed sheet (Fig. 1) then at $X = X_1$

$$u = u_1 \quad \text{(prescribed)}$$

and
$$\sigma_{XY} = 0 \tag{2-52}$$

and at $Y = Y_1$

$$v = v_1 \quad \text{(prescribed)}$$

and
$$\sigma_{XY} = 0 \tag{2-53}$$

It is assumed that the sides $X = X_1$ and $Y = Y_1$ are far enough from the hole so that we can replace the shearing stress conditions by the linear displacement conditions,

$$v = \frac{Y}{Y_1} v_1 \quad ; \quad u = \frac{X}{X_1} u_1 \tag{2-54}$$

The hole is free of traction so that

$$\sigma_{XX} \ell + \sigma_{XY} m = 0$$

$$\sigma_{XY} \ell + \sigma_{YY} m = 0 \tag{2-55}$$

where the direction cosines of the unit normal are

$$\ell = \cos(N,X) = \frac{dX}{dN} = \frac{dY}{dS}$$

$$m = \cos(N,Y) = \frac{dY}{dN} = \frac{-dX}{dS} \tag{2-56}$$

By substituting Eqs. (2-56) into (2-55), the boundary conditions along the hole can be written as

$$\sigma_{XX}\frac{dY}{dS} - \sigma_{XY}\frac{dX}{dS} = 0$$

$$\sigma_{XY}\frac{dY}{dS} - \sigma_{YY}\frac{dX}{dS} = 0 \qquad (2\text{-}57)$$

where the stresses can be expressed in terms of the derivatives of the displacements by utilizing Eqs. (2-36) and (2-41). The piecewise linear form of the stress-displacement relationship can then be expressed as

$$a\sigma_{XX} = a_1\Delta u_{,1} + a_2\Delta u_{,2} + b_1\Delta v_{,1} + b_2\Delta v_{,2} + k_1$$

$$a\sigma_{YY} = d_1\Delta u_{,1} + d_2\Delta u_{,2} + e_1\Delta v_{,1} + e_2\Delta v_{,2} + k_2 \qquad (2\text{-}58)$$

$$a\sigma_{XY} = f_1\Delta u_{,1} + f_2\Delta u_{,2} + g_1\Delta v_{,1} + g_2\Delta v_{,2} + k_3$$

where a_1, a_2, b_1, b_2, k_1, d_1, d_2, e_1, e_2, k_2 and f_1, f_2, g_1, g_2, k_3 are given in Appendix A.

The procedure for evaluating $\frac{dX}{dS}$, $\frac{dY}{dS}$ is as follows. The hole is delineated by placing evenly spaced particles on the boundary curve. These particles then trace the boundary throughout the deformation process. The derivatives $\frac{dX}{dS}$, $\frac{dY}{dS}$ at a particular boundary particle i is obtained by expressing $X = X(S)$ and $Y = Y(S)$ at the points $i-1$ and $i+1$ by a Taylor series expansion about point i (Fig. 2) and retaining only terms up to the third order. The solution of the two simultaneous equations then results in the following expressions

$$\frac{dX}{dS}(i) = \frac{X(i+1)(S_{i-1,i})^2 - X(i-1)(S_{i,i+1})^2 + X(i)[(S_{i,i+1})^2 - (S_{i-1,i})^2]}{S_{i-1,i}\,S_{i,i+1}\,(S_{i-1,i} + S_{i,i+1})} + O(S^2)$$

$$\frac{dY}{dS}(i) = \frac{Y(i+1)(S_{i-1,i})^2 - Y(i-1)(S_{i,i+1})^2 + Y(i)[(S_{i,i+1})^2 - (S_{i-1,i})^2]}{S_{i-1,i}\,S_{i,i+1}\,(S_{i-1,i} + S_{i,i+1})} + O(S^2) \qquad (2\text{-}59)$$

where

$$S_{i-1,i} = \{[X(i) - X(i-1)]^2 + [Y(i) - Y(i-1)]^2\}^{\frac{1}{2}}$$
$$S_{i,i+1} = \{[X(i+1) - X(i)]^2 + [Y(i+1) - Y(i)]^2\}^{\frac{1}{2}} \qquad (2\text{-}60)$$

The partial derivatives in the linearized stress displacement relations, Eqs. (2-58), must be expressed in forward difference form at the boundary of the hole and are, for example,

$$u,_1(i,j) = \frac{1}{2k}[-3u(i,j) + 4u(i+k,j) - u(i+2k,j)] + 0(k^2)$$
$$u,_2(i,j) = \frac{1}{2k}[-3u(i,j) + 4u(i,j+k) - u(i,j+2k)] + 0(k^2) \qquad (2\text{-}61)$$

The linearized finite difference form of the traction free boundary may then be expressed as

$$\ell_1\Delta u(i,j)+\ell_2\Delta u(i+k,j)+\ell_3\Delta u(i+2k,j)+\ell_4\Delta u(i,j+k)+\ell_5\Delta u(i,j+2k)$$
$$+ m_1\Delta v(i,j)+m_2\Delta v(i+k,j)+m_3\Delta v(i+2k,j)+m_4\Delta v(i,j+k)+m_5\Delta v(i,j+2k)$$
$$+ k_4 = 0 \qquad (2\text{-}62a)$$

$$n_1\Delta u(i,j)+n_2\Delta u(i+k,j)+n_3\Delta u(i+2k,j)+n_4\Delta u(i,j+k)+n_5\Delta u(i,j+2k)$$
$$+ p_1\Delta v(i,j)+p_2\Delta v(i+k,j)+p_3\Delta v(i+2k,j)+p_4\Delta v(i,j+k)+p_5\Delta v(i,j+2k)$$
$$+ k_5 = 0 \qquad (2\text{-}62b)$$

where

$$\ell_1 = \frac{3}{2k}\left[(f_1 + f_2)\frac{dX}{dS}(i,j) - (a_1 + a_2)\frac{dY}{dS}(i,j)\right]$$
$$\ell_2 = \frac{2}{k}\left[a_1\frac{dY}{dS}(i,j) - f_1\frac{dX}{dS}(i,j)\right]$$

(continued on next page)

$$l_3 = \frac{1}{2k}\left[f_1 \frac{dX}{dS}(i,j) - a_1 \frac{dY}{dS}(i,j)\right]$$

$$l_4 = \frac{2}{k}\left[a_2 \frac{dY}{dS}(i,j) - f_2 \frac{dX}{dS}(i,j)\right]$$

$$l_5 = \frac{1}{2k}\left[f_2 \frac{dX}{dS}(i,j) - a_2 \frac{dY}{dS}(i,j)\right]$$

$$m_1 = \frac{3}{2k}\left[(g_1 + g_2) \frac{dX}{dS}(i,j) - (b_1 + b_2) \frac{dY}{dS}(i,j)\right]$$

$$m_2 = \frac{2}{k}\left[b_1 \frac{dY}{dS}(i,j) - g_1 \frac{dX}{dS}(i,j)\right]$$

$$m_3 = \frac{1}{2k}\left[g_1 \frac{dX}{dS}(i,j) - b_1 \frac{dY}{dS}(i,j)\right]$$

$$m_4 = \frac{2}{k}\left[b_2 \frac{dY}{dS}(i,j) - g_2 \frac{dX}{dS}(i,j)\right]$$

$$m_5 = \frac{1}{2k}\left[g_2 \frac{dX}{dS}(i,j) - b_2 \frac{dY}{dS}(i,j)\right]$$

$$k_4 = k_1 \frac{dY}{dS}(i,j) - k_3 \frac{dX}{dS}(i,j)$$

$$n_1 = \frac{3}{2k}\left[(d_1 + d_2) \frac{dX}{dS}(i,j) - (f_1 + f_2) \frac{dY}{dS}(i,j)\right]$$

$$n_2 = \frac{2}{k}\left[f_1 \frac{dY}{dS}(i,j) - d_1 \frac{dX}{dS}(i,j)\right]$$

$$n_3 = \frac{1}{2k}\left[d_1 \frac{dX}{dS}(i,j) - f_1 \frac{dY}{dS}(i,j)\right]$$

$$n_4 = \frac{2}{k}\left[f_2 \frac{dY}{dS}(i,j) - d_2 \frac{dX}{dS}(i,j)\right]$$

$$n_5 = \frac{1}{2k}\left[d_2 \frac{dX}{dS}(i,j) - f_2 \frac{dY}{dS}(i,j)\right]$$

$$p_1 = \frac{3}{2k}\left[(e_1 + e_2)\frac{dX}{dS}(i,j) - (g_1 + g_2)\frac{dY}{dS}(i,j)\right]$$

$$p_2 = \frac{2}{k}\left[g_1\frac{dY}{dS}(i,j) - e_1\frac{dX}{dS}(i,j)\right]$$

$$p_3 = \frac{1}{2k}\left[e_1\frac{dX}{dS}(i,j) - g_1\frac{dY}{dS}(i,j)\right]$$

$$p_4 = \frac{2}{k}\left[g_2\frac{dY}{dS}(i,j) - e_2\frac{dX}{dS}(i,j)\right]$$

$$p_5 = \frac{1}{2k}\left[e_2\frac{dX}{dS}(i,j) - g_2\frac{dY}{dS}(i,j)\right]$$

$$k_5 = k_3\frac{dY}{dS}(i,j) - k_2\frac{dX}{dS}(i,j) \qquad (2\text{-}63)$$

The values of $\frac{dX}{dS}(i,j)$, $\frac{dY}{dS}(i,j)$ at the center of each boundary cell are obtained by averaging the values of the derivatives of all of the boundary particles lying in the cell at any step. Again, it should be noted that the boundary conditions at each incremental step are satisfied in the same sense as they are in classical elasticity theory.

G. Extension of a Thin Elastic Sheet with a Rigid Inclusion at its Center

We consider a rectangular sheet subjected to biaxial extensions, and having a rigid inclusion at its center. The inclusion is of arbitrary shape; however, since we desire to consider only one quarter of the sheet, symmetry of the inclusion is required. The previous formulation for the traction free hole remains unchanged except for the boundary conditions at the hole, Eqs. (2-57), which is now replaced by the statement that

$$u = v = 0$$

at the interface.

H. The Computer Program and the Computation Procedure

The program described here was written in fortran language and run on an IBM 360, model 50, computer. In its present form it represents the basic program necessary to solve the problems described. No auxiliary storage facilities are used and the program is presently limited, because of the machine storage capacity, to solutions of small finite deformations. In order to be able to exceed the present range it is necessary to include enough auxiliary storage units so that it will be possible to include the new cells which are required as the deformation progresses. It is also necessary to use a machine which retains more significant figures since the loss of significant figures is quite rapid in solutions of large matrices such as those encountered here.

The program consists of a main program and a set of subroutines. The main program reads in data, prints output, and controls the subroutines. The parameters of the problem are read into the main program by data cards and can be changed as desired. These parameters consist of the spacing k, the initial dimensions of the sheet and its material coefficients, the shape of the hole, the size of displacement increments and the number of incremental steps, and the spacing of the distributed particles.

The computation proceeds by first calling for the subroutine which distributes the particles throughout the sheet and along the boundary of the hole. This step is followed by a scanning subroutine which scans the region of the hole and determines the location of the boundary cells, which are defined as cells which contain one or more of the boundary particles. The main program next calls for the subroutine which calculates the derivatives $\frac{dX}{dS}$, $\frac{dY}{dS}$ at each of the boundary particles and then attributes to the boundary cell in which they lie, their average values. This is then followed by a subroutine which calculates the coefficients of the linear algebraic simultaneous equations arising from the finite difference solution of the piecewise linearized forms of the equilibrium equations (2-49) and the boundary conditions (2-62). The same subroutine also calculates the stresses at the end of each step.

Both an iterative and direct method were used to solve the simultaneous equations. The iterative method used is the S.O.R. which can be described briefly as follows. Consider an $n \times n$ matrix $A = (a_{ij})$ which is nonsingular and with nonzero diagonal elements. We seek the solution of the system of linear equations

$$Ax = K$$

or

$$\sum_{j=1}^{n} a_{ij} x_j = k_i \qquad 1 \leq i \leq n \tag{2-64}$$

The S.O.R. iteration process is given by the following algorithm[38]

$$x_i^{(m+1)} = x_i^{(m)} + \omega\{-\frac{1}{a_{ii}}\sum_{j=1}^{i-1} a_{ij}x_j^{(m+1)} - \frac{1}{a_{ii}}\sum_{j=i+1}^{n} a_{ij}x_j^{(m)} + \frac{k_i}{a_{ii}} - x_i^{(m)}\} \tag{2-65}$$

where ω is the relaxation factor and (m), $(m+1)$ indicate the m^{th} and $(m+1)^{th}$ iteration respectively. When $\omega = 1$ the S.O.R. method is identical with the Gauss-Seidel iteration method.

When iteration is used, parameters such as maximum error and number of iterations allowed have to be read in. Starting with assumed initial distribution of Δu, Δv, the iteration is carried out by moving along pivotal points which lie along lines parallel to one of the symmetry axes, with Δu calculated first, followed by the calculations of Δv at the same pivotal point. Proceeding from the outer boundary towards the hole or in the opposite direction gave similar rates of convergence.

The direct method used is based on the Gauss elimination with pivotal condensation[39]. First we select the largest element of the coefficient matrix A, say a_{kj}, which is called the pivot. A multiplier $m_i = -a_{ij}/a_{kj}$ is then computed for each row $i \neq k$. Next, the k^{th} row is multiplied by m_i and added to the i^{th} row. This leads to a new matrix with zeros in the j^{th} column, except for a_{kj}. The same process is now repeated for the auxiliary matrix which excludes the j^{th} column and the k^{th} row. The process yields an upper diagonal matrix which can be written with unit entries along its main diagonal. The solution is obtained by going from the last row of the upper diagonal matrix to the first and in each row substituting all the known values and trans-

ferring all terms off the main diagonal to the right hand side. Thus the values of the right hand side yield the solution. The disadvantage of this procedure is the rapid loss of significant figures which occurs for large matrices.

The IBM GELB subroutine was used to carry out the direct method. This subroutine is written for solution of banded matrices. It uses Gaussian elimination with column pivoting only. The subroutine GELB requires that the elements of the matrix be stored row after row as a one dimensional array. Therefore, GELB is preceeded by a subroutine which arranges the elements of the matrices in the proper order.

The solution of the simultaneous equations yields Δu and Δv of each cell center. Next, a subroutine is called for which computes the total displacements of each particle, their new coordinates and cells in which they lie. The new boundary cells are then found, and the magnitude of the displacements associated with the cell centers are recalculated. This completes the computations for the first increment. Further steps are computed by reading in the new prescribed end displacement increments and repeating the general procedure described above.

The program was also adopted to the solution of the problem of the rigid inclusion in a sheet. It contains all the elements of the hole program, with the exception that no derivatives are calculated along the interface and that the boundary cells,of course, remain fixed.

3. EXPERIMENTS

A. Experimental Equipment

A biaxial testing apparatus, designed by the author, was used to conduct the biaxial experiments. It consists of a loading mechanism, an environmental chamber and control and measuring instruments (Fig. 3). The loading mechanism consists of an electric motor (1/2 H.P.) connected to four shafts through a conical gear transmission. The shafts are thus driven simultaneously and have identical speeds. Each shaft is connected to two parallel driving screws by means of sprockets and chains, resulting in movement of the four crossheads, which in turn transmit their motion to the specimen through a loading frame. The stretching mechanism thus ensures that the center of the specimen is always stationary and therefore always remains centered. Crosshead speeds in the two principal directions can be varied independently by adjusting the gear ratios in the chain-sprocket assembly. A range of crosshead speeds from 1 to 20 in/min can be obtained by a suitable adjustment of the sprocket assembly and motor speed. Each crosshead has a travelling range of 15 in.

The test specimen (a rectangular thin sheet) was cut so that a series of lugs was formed on each of its sides. Each of these lugs was connected to a light aluminum end strip which is pinned to a roller, consisting of a miniature ball bearing mounted in an aluminum U-section.

The rollers are constrained to move along the rails of the aluminum loading frames (Fig. 4), each side of which is connected to the crosshead by twin parallel rods which pass through special low friction guides. The lengths of the rods are adjustable for use with different size specimens. Out of plane or lateral motions are prevented by supporting the loading frames on rollers which rest on an adjustable support platform. Loads are measured by placing load cells between the guide rods and the crossheads.

The environmental chamber is an insulated box, having test chamber dimensions of 30 x 30 x 12 inches. Cooling coils and strip heaters are attached along the side walls and four small fans are used for air circulation, so as to maintain a uniform temperature throughout the chamber. The cooling is done by connecting the coils to a 1 1/2 H.P. Bendix-Westinghouse Co. low temperature compressor, and supplementing this by using liquid nitrogen for the very low temperatures. A range of temperature from -80 to 200^{o}F can be achieved with variation of $\pm$ 1^{o}F throughout the test chamber. Temperature is controlled by a West Instrument Corp. Gardsman control unit which controls the strip heaters. Below room temperatures are reached by operating the compressor continuously and controlling the heat input of the heaters. It was found that this operating procedure results in a more stable temperature than when both heating and cooling rates or only cooling rates are controlled. The upper surface of the environmental chamber is covered by a thermal pane, free to move along two support rails, thereby permitting optical measurements of the displacements of the test piece, as well as easy access to the chamber interior.

Some uniaxial experiments were also conducted. The equipment used for these tests consists of a Universal Testing Instrument Model TTC Ml.3 made by Instron Engineering Corporation, and an FRL Environmental Box designed by Fabric Research Laboratories. Heating in the chamber is accomplished by use of strip heaters, and cooling is done by use of either dry ice or liquid nitrogen. A Barber-Colman Co. Wheelco unit provides temperature control over a range of -100 to 400°F by operating the strip heaters.

B. Specimen Preparation

The experiments were performed on specimens of natural rubber (cured with 1 part of di cumyl peroxide, 2.5 pt dicup 40c) all of which were cut from the same sheet in order to reduce possible variations of the material properties. The thickness of the sheet was 0.079 ± 0.004 in. A specimen having 6 1/2 in. sides was used for the biaxial experiments, and a strip having a length of 5 in. and a width of 0.375 in. was used for the uniaxial tests.

For the biaxial experiments a silk screen was prepared having sub-divisions varying from 1/4 in. at its perimeter to 1/32 in. in its interior. Although the small sub-divisions were not required for the characterization experiments, they were necessary for the stress concentration experiments which were carried out on the same sheet.

The grid was printed on the specimen by placing the screen over it and spreading a rubber base ink (Ridgway RC 1154, R.I. White) over the surface of the screen by pressing a squeegee over it.

C. Experimental Procedure

The specimen was placed in the loading rig and stretched to a predetermined elongation in one direction. This elongation was then kept fixed while the perpendicular sides were stretched over a range of elongation ratios from 1.0 to 1.8 in 0.1 steps. The procedure was repeated for different values of the fixed elongation. Isotropy in the undeformed state was checked by repeating the tests with interchanged principal axes, and noting that there was only a slight variation in loads corresponding to interchanged elongations. Before each test the specimen was relaxed for two hours at the highest temperature of the tests ($150^{\circ}F$) in order to release possible residual stresses.

The experiments were performed at 30, 60, 90, 120 and $150^{\circ}F$. Only slight temperature effects could be detected in the biaxial experiments, and since these were within the experimental error, temperature effects could not be isolated.

The displacements of the sheet were recorded at prescribed crosshead positions by photographing the specimen with a 4 X 5 in. view camera (made by Calumet Manufacturing Co.) mounted on a tripod placed on the thermal pane cover (Fig. 5). By using high contrast film the image on the negative appears as sharp black lines on a clear background. A typical negative is shown in Fig. 6. The scales of the negatives were determined by placing a standard ruler in the plane of the specimen while photographing. Distances between grid lines were determined by scanning the negatives with a microdensitometer (made by Joyce, Loebl and Co., England) or an x-y micrometer table mounted

on a precision transmission polariscope (made by Photoelastic Inc.). Measuring sensitivities of both instruments were at least of the order of .0001 in. The undeformed specimen was similarly analyzed and thus displacements and elongation ratios were determined.

The biaxial tests were supplemented by a series of uniaxial tests. A strip cut from the same sheet was tested at temperatures varying from 30 to 150°F. Temperature effects in the uniaxial tests were more pronounced than those observed in the biaxial experiments.

After completion of the material characterization experiments a 0.5 in. diameter hole was punched in the center of the sheet. A series of stress concentration experiments were conducted at 90°F, using the same experimental procedure as described. A typical photograph of the deformed specimen is shown in Fig. 7.

D. Material Characterization Experiments

i) Analytical Analysis

Consider a thin rectangular plane sheet of uniform thickness having edges parallel to the x and y axes. The sheet is subjected to a pure homogeneous deformation having principal directions parallel to the x, y and z axes.

Let λ_1, λ_2, λ_3 be the principal extention ratios, defined as the ratios, in the principal directions, of final length to original lengths of the elements

$$\lambda = \ell_f/\ell_o \tag{3-1}$$

The sheet is assumed to be isotropic and incompressible, so that the constitutive equations can be expressed as follows[3]

$$\sigma_{ii} = 2(\lambda_i^2 \frac{\partial W}{\partial I_1} - \frac{1}{\lambda_i^2} \frac{\partial W}{\partial I_2}) + p \qquad (i = 1,2,3 \text{ or } x,y,z) \tag{3-2}$$

where σ_{ii} is the principal true stress and p is an arbitrary hydrostatic pressure. The strain energy function W is expressible as a function of the invariants I_1, I_2, which, in terms of the principal extension ratios, are

$$I_1 = \lambda_1^2 + \lambda_2^2 + 1/\lambda_1^2\lambda_2^2 \tag{3-3}$$

$$I_2 = 1/\lambda_1^2 + 1/\lambda_2^2 + \lambda_1^2\lambda_2^2$$

Since $\sigma_{33} = 0$ we can solve for p and rewrite Eqs. (3-2) as

$$\sigma_{11} = 2(\lambda_1^2 - 1/\lambda_1^2\lambda_2^2)(\frac{\partial W}{\partial I_1} + \lambda_2^2 \frac{\partial W}{\partial I_2})$$

$$\sigma_{22} = 2(\lambda_2^2 - 1/\lambda_1^2\lambda_2^2)(\frac{\partial W}{\partial I_1} + \lambda_1^2 \frac{\partial W}{\partial I_2}) \tag{3-4}$$

Solving for $\frac{\partial W}{\partial I_1}$, $\frac{\partial W}{\partial I_2}$ from Eq. (3-4) yields

$$\frac{\partial W}{\partial I_1} = \frac{\left[\frac{\lambda_1^2 \sigma_{11}}{\lambda_1^2 - 1/\lambda_1^2\lambda_2^2} - \frac{\lambda_2^2 \sigma_{22}}{\lambda_2^2 - 1/\lambda_1^2\lambda_2^2}\right]}{2(\lambda_1^2 - \lambda_2^2)} \tag{3-5a}$$

and $$\frac{\partial W}{\partial I_2} = \frac{-\left[\frac{\sigma_{11}}{\lambda_1^2 - 1/\lambda_1^2\lambda_2^2} - \frac{\sigma_{22}}{\lambda_2^2 - 1/\lambda_1^2\lambda_2^2}\right]}{2(\lambda_2^2 - \lambda_1^2)} \tag{3-5b}$$

The true stress can be expressed as

$$\sigma_{11} = \frac{\lambda_1 F_1}{\ell_2 h_o} \quad \text{and} \quad \sigma_{22} = \frac{\lambda_2 F_2}{\ell_1 h_o} \tag{3-6}$$

where the F_i's are the total loads acting along the sides of undeformed lengths ℓ_i and h_o is the thickness of the undeformed sheet. The loads F_i are assumed to be evenly distributed along the sides of the specimen. Experimental errors in measuring σ_{11} and σ_{22} affect Eq. (3-5b) more seriously than Eq. (3-5a). To reduce the errors, the smaller stress, say σ_{11}, was eliminated from Eq. (3-5b), and $\partial W/\partial I_2$ was determined from the resulting expression

$$\frac{\partial W}{\partial I_2} = \left[\frac{\sigma_{22}}{2(\lambda_2^2 - 1/\lambda_1^2\lambda_2^2)} + \frac{\partial W}{\partial I_1}\right] \Big/ \lambda_1^2 \tag{3-7}$$

For the case of uniaxial extension parallel to the x-axis

$$\lambda_2^2 = 1/\lambda_1 \tag{3-8}$$

and Eq. (3-4) becomes

$$\sigma_{11} = 2(\lambda_1^2 - \frac{1}{\lambda_1})(\frac{\partial W}{\partial I_1} + \frac{1}{\lambda_1}\frac{\partial W}{\partial I_2}) \tag{3-9}$$

ii) Experimental Results

The biaxial tests were conducted by keeping one of the extension ratios fixed and varying the other. From these experiments the stresses were determined as functions of the extension ratios, λ_1 and λ_2, and thus as functions of the invariants, I_1 and I_2. These values were used in Eqs. (3-5a) and (3-7) to determine $\frac{\partial W}{\partial I_1}$ and $\frac{\partial W}{\partial I_2}$ as functions of I_1 and I_2. Plots of $\frac{\partial W}{\partial I_1}$ as a function of I_1 and I_2 are shown in Figs. 8. It is seen that within the experimental error $\frac{\partial W}{\partial I_1}$ is independent of both I_1 and I_2, and is equal to the constant $C_1 = 20.28$ psi. Similar plots of $\frac{\partial W}{\partial I_2}$ as a function of I_1 and I_2 are given in Figs. 9. In Fig. 9a we observe that a reasonable fit to the data is that $\frac{\partial W}{\partial I_2}$ is independent of I_1, and Fig. 9b shows that its value decreases with increasing values of I_2. A least square parabolic fit to the data yields the function:

$$\frac{\partial W}{\partial I_2} = [5.808 - 1.440\ (I_2 - 3) + 0.1379\ (I_2 - 3)^2]\ \text{psi} \qquad (3\text{-}10)$$

which is shown as a solid curve in Fig. 9b. Thus we may express the strain energy function as

$$W = 20.28(I_1 - 3) + 5.808(I_2 - 3) - \frac{1.440}{2}\ (I_2 - 3)^2 + \frac{0.1379}{3}\ (I_2 - 3)^3 \qquad (3\text{-}11)$$

It should be noted that this form has been obtained from data in the low ranges of I_1 and I_2, i.e., I_1 and $I_2 < 8$.

Since the stress concentration experiments will be conducted so that the maximum values of I_1 and I_2 are within this range, these low range results will be applicable.

Uniaxial extension tests were conducted at 30, 60, 90, 120 and 150°F. The results show (Fig. 10) that the material becomes stiffer with increasing temperature, a result which is in agreement with the kinetic theory for rubber elasticity.

Fig. 11 shows a plot of the uniaxial stress as a function of elongation ratio at a temperature of 90°F. The solid line has been determined by using the form of the strain energy function obtained from the biaxial experiments and substituting it into Eq. (3-9).

4. NUMERICAL CALCULATIONS

The modified P.I.C. method was applied to the problems of a circular hole and a rigid inclusion in a sheet. Preliminary calculations were performed on the former problem by assuming a 4 x 4 unit square sheet having a circular hole of radius r_o = 1 unit. A 2o x 2o grid (k = 0.20) was used, thus resulting in approximately 800 simultaneous equations (u,v are unknown at each cell center). The equations were so arranged that a diagonally banded matrix containing over 100 elements was obtained. Both direct and iterative methods were applied. Difficulties with convergence of the S.O.R. iterative scheme arose, while in the direct method (Gaussion elimination with column pivoting) a great many significient figures were lost after several incremental steps. While results showed agreement with the linear theory for the first few incremental steps, no meaningful results could be obtained for finite deformations.

For the rigid inclusion problem the displacement boundary conditions did not result in a complication of the matrix, as did the stress free boundary conditions of the former case. A 10 x 10 grid (k = 0.3) was used, and the direct method of solution yielded reasonable results. Since the displacement functions were much smoother for the case of the rigid inclusion than for the case of the cutout, it is to be expected that a courser grid could be successfully applied to the former problem.

It should be pointed out that the analytical development of the linearized equations of motion (2-47) was carried out under the assumption

that the material could be described by the Rivlin-Mooney constitutive equations. However, the results of the experiments on the natural rubber indicate that the material is described by Eq. (3-11), and thus will be referred to as a Generalized Rivlin-Mooney material. To make these two results compatible, it was decided that in the analytical work, C_2 would be chosen to be a function of I_2 as shown in Fig. (9b), that is, it was assumed that $C_2 = \partial W(I_2)/\partial I_2$

5. DISCUSSION

The results of the material characterization experiments on a thin sheet of natural rubber are presented in Figs. (8-11). Figs.(8) show that $\partial W/\partial I_1$ is independent of the strain invariants I_1, I_2, and has a value $C_1 = 20.28$ psi. Similar graphs for $\partial W/\partial I_2$ are found in Figs.(9), which indicate that $\partial W/\partial I_2$ is independent of I_1 and decreases with increasing values of I_2. It should be noted that the form of the strain energy function (3-11) has been obtained from data in the low ranges of I_1 and I_2, i.e. for I_1, $I_2 < 8$. Since the stress concentration experiments were conducted so that the maximum values of I_1 and I_2 fall within this range, these low range results are applicable.

At the completion of the material characterization experiments a circular hole was cut at the center of the sheet. A series of biaxial experiments were then performed on the specimen at a temperature of 90^{o}F. Fig. 12 shows the experimentally obtained displacements along the axis of symmetry (x=o) for the equi-biaxial elongations. Investigation of the slopes in the vicinity of $y/r_o = 13.0$ indicates that, essentially, an isotropic strain state exists there. Thus the results obtained are not very different from those that would be obtained from an infinite sheet. It is for this reason that the ratio of the deformed to the undeformed length of the membrane is designated λ_∞ ($= X_1/x_1 = Y_1/y_1$) for the equi-biaxial case. For the general biaxial state $(\lambda_x)_\infty$ and $(\lambda_y)_\infty$ refer to

the length ratios in the x- and y directions, respectively. Displacements for the uni-directional extension, i.e. $(\lambda_x)_\infty = 1.0$, are presented in Figs. 13, and the corresponding deformed shapes of the hole are shown in Fig. 14. Substituting the displacements and their derivatives into the constitutive equations (2-36) results in the experimentally determined stresses. The stress σ_{yy} (circumferential) at the intersection of the hole and the x - axis is plotted in Fig. 15. A comparison with linear theory indicates that no significant deviation occurs until $\lambda_\infty > 1.3$. A plot of the stress concentration factor K_t is presented in Fig. 16, where it is seen that the factor varies from 2.0 for small strains to approximately 4.0 at $\lambda = 1.6$.

No analytical results were obtained for the problem of the hole in the sheet for reasons which are discussed in Chapter IV. Although no experiments were performed on the sheet containing a rigid inclusion, the modified Particle - in - Cell (P.I.C.) method was applied to the problem. The results for the equi-biaxial case are presented in Figs. 17-20. The stress concentration factor K_r, is presented in Fig. 20 for a Generalized Rivlin-Mooney (3-11), a Rivlin-Mooney (2-33) and a linear elastic material. The curves indicate that the stress concentration factor decreases with an increase in λ_∞ for the Generalized Rivlin-Mooney material, while for a Rivlin-Mooney material the situation is reversed. The results for the Rivlin-Mooney material agree qualitatively with those obtained by Yang [32], and with those obtained from an analysis of the displacements presented by Rivlin and Thomas [31].

REFERENCES

1. Murnaghan, F. D., "Finite Deformation of an Elastic Solid", John Wiley and Son, Inc., New York 1951.

2. Rivlin, R. S., "Large Elastic Deformations of Isotropic Materials, I. Fundamental Concepts". Phil. Trans., Vol. A 240, pp. 459-490, 1948.

3. Rivlin, R. S., "Large Elastic Deformations of Isotropic Materials, IV. Further Developments of the General Theory". Phil. Trans., Vol. A 241, pp. 379-397, 1948.

4. Treloar, L. R. G., "The Physics of Rubber Elasticity", edn. 2, Clarendon Press, Oxford, 1958.

5. Novozhilov, V. V., "Foundations of the Nonlinear Theory of Elasticity", Graylock Press, Rochester, New York, 1953.

6. Green, A. E. and Shield, R. T., "Finite Deformation of Incompressible Isotropic Bodies", Proc. Roy. Soc., Vol. A 202, pp. 407-419, 1950.

7. Green, A. E. and Zerna, W., "Theoretical Elasticity", Clarendon Press, Oxford, 1954.

8. Mooney, M. J., "A Theory of Large Deformation", J. Appl. Physics, Vol. 11, pp. 582-592, 1940.

9. Truesdell, C., "The Mechanical Foundations of Elasticity and Fluid Dynamics", J. Rat. Mech. Anal., Vol. 1, pp. 125-300, 1952, and Vol. 2, pp. 593-616, 1953.

10. Green, A. E. and Adkins, J. E., "Large Elastic Deformations and Nonlinear Continuum Mechanics", Clarendon Press, Oxford, 1960.

11. Ericksen, J. L. and Rivlin, R. S., "Large Elastic Deformations of Homogeneous Anisotropic Materials", J. Rat. Mech. Anal., Vol. 3, pp. 281-301, 1954.

12. Ericksen, J. L., "Inversion of a Perfectly Elastic Spherical Shell", ZAMP, Vol. 35, pp. 382-385, 1955.

13. Green, A. E. and Wilkes, E. W., "Finite Plane Strain for Orthotropic Bodies", J. Rat. Mech. Anal., Vol. 3, pp. 713-723, 1954.

14. Green, A. E., "Finite Elastic Deformation of Compressible Isotropic Bodies", Proc. Roy. Soc., Vol. A 227, pp. 271-278, 1955.

15. Adkins, J. E., "Some General Results in the Theory of Large Elastic Deformations", Proc. Roy. Soc., Vol. A 231, pp. 75-90, 1955.

16. Adkins, J. E., "A Note on the Finite Plane Strain Equations for Isotropic Incompressible Materials", Proc. Camb. Phil. Soc., Vol. 51, pp. 363-367, 1955.

17. Green, A. E. and Shield, R. T., "Finite Extension and Torsion of Cylinders", Phil. Trans., Vol. A 244, pp. 47-86, 1951.

18. Blatz, P. J., "Finite Elastic Deformation of a Plane Strain Wedge-Shaped Radial Crack in a Compressible Cylinder", Int. Symp. on Nonlinear Diff. Eqs. and Nonlinear Mechanics, Air Force Academy, Colorado Springs, Colorado, Aug. 2, 1961.

19. Muskhelishvili, N. I., "Some Basic Problems of the Mathematical Theory of Elasticity", Translated from Russian by J.R.M. Radck, Groningen, Holland, P. Noordhoff Ltd., 1963.

20. Savin, G. N., "Stress Concentration Around Holes, Translated from Russian by W. Johnson, Pergamon Press, London, 1961.

21. Sternberg, E., "Three Dimensional Stress Concentrations in the Theory of Elasticity", Appl. Mech. Rev., Vol. 11, pp. 1-4, 1958.

22. Neuber, H. and Hahn, H. G., "Stress Concentration in Scientific Research and Engineering", Appl. Mech. Rev., Vol. 19, pp. 187-199, 1966.

23. Sheng, P. L., "Secondary Elasticity", Taipei, 1955.

24. Rivlin, R. S. "The Solutions of Problems in Second Order Elastic Theory", J. Rat. Mech. Anal., Vol. 2, pp. 53-81, 1953.

25. Carlson, D. E. and Shield, R. T., "Second and Higher Order Effects in a Class of Problems in Plane Finite Elasticity", Arch. Rat. Mech. Anal., Vol. 19, pp. 189-214, 1965.

26. Adkins, J. E. and Green, A. E., "Plane Problems in Second Order Theory", Proc. Roy. Soc., Vol. A 239, pp. 557-576, 1957.

27. Adkins, J. E., Green, A. E. and Nicholas, G. C., "Two-Dimensional Theory of Elasticity for Finite Deformations", Phil. Trans., Vol. A 247, pp. 279-306, 1954.

28. Adkins, J. E., Green, A. E. and Shield, R. T., "Finite Plane Strain", Phil. Trans., Vol. A 246, pp. 181-213, 1953.

29. Guz', A. N., Savin, G. N. and Tsurpal, I. A., "Stress Concentration About Curvilinear Holes in Physically Nonlinear Elastic Plates", NASA Technical Translation TT, F-408, Washington, D.C., January 1966.

30. Evans, R. J. and Pister, K. S , "Constitutive Equations for a Class of Nonlinear Elastic Solids", Int. J. Solids Structures, Vol. 2, pp. 427-445, 1966.

31. Rivlin, R. S. and Thomas, A. G., "Large Elastic Deformations of Isotropic Materials, VIII. Strain Distribution Around a Hole in a Sheet", Phil. Trans., Vol. A 243, pp. 289-298, 1951.

32. Yang, W. H., "Stress Concentration in a Rubber Sheet Under Axially Symmetric Stretching", J. Appl. Mech., Vol. 34, pp. 942-946, 1967.

33. Baron, M. L., Skalak, R. and Lecht, C. P., "Particle-In-Cell Method Studies and Their Applications", ASCE J. of Eng. Mech. Div., Vol. 91, EM 3, pp. 129-146 , 1965.

34. Baron, M. L., Christian, C. E. and Skidan, O., "Particle-In-Cell Method Studies in Shock Propagation Problems", ASCE J. Eng. Mechs. Div., Vol. 92, EM 6, pp. 205-228, 1966.

35. Harlow, F. H., "The Particle-In-Cell Method for Two-Dimensional Hydrodynamic Problems", Rept. No. LAMS-2082, Los Alamos Scientific Lab., Los Alamos, N. Mexico, December 1956.

36. Brode, H. L. and Bjork, R. L., "Cratering from a Megaton Surface Burst", Research Memorandum, No. RM-2500, The RAND Corp., June 30, 1960.

37. Rivlin, R. S. and Saunders, D. W., "Large Elastic Deformations of Isotropic Materials, VII. Experiments on the Deformation of Rubber", Phil. Trans., Vol A 243, pp. 251-288, 1951.

38. Varga, R. S., "Matrix Iterative Analysis", Prentice-Hall, Inc., Englewood Cliffs, New Jersey, 1962.

39. Faddeeva, V. N., "Computational Methods of Linear Algebra", Dover Publications, Inc., New York, 1959.

APPENDIX A

COEFFICIENTS OF LINEARIZED EQUILIBRIUM AND STRESS-DISPLACEMENT EQUATIONS

Let the displacements at the end of the n-th step be denoted by u and v. The coefficients of the linearized equations at the (n + 1)-th step are then given by the following expressions.

i) Coefficients of Linearized Equilibrium Equations (2-47)

$$
\begin{aligned}
A_1 = \; & -C\,[2V(1-u_{,1}) + 2U u_{,2} + 3L^4 v_{,12} + 12 L^3 M (1 - v_{,2})] \\
& + L\,\{-2L\,[3(1-u_{,1})(1-v_{,2}) - u_{,2} v_{,1}]\, u_{,11} - 2S(1-v_{,2})\, u_{,11} \\
& + 2L\,[(1-v_{,2})\, u_{,2} - (1-u_{,1})\, v_{,1}]\, u_{,12} - 2N(1-v_{,2})\, u_{,12} - 2L^2 u_{,22} \\
& - 2Z(1-v_{,2})\, u_{,22} + 2L\,[(1-v_{,2})\, v_{,1} - (1-u_{,1})\, u_{,2}]\, v_{,11} \\
& - 2P(1-v_{,2})\, v_{,11} + L[(u_{,2})^2 - 3(1-u_{,1})^2 - (v_{,1})^2 - (1-v_{,2})^2]\, v_{,12} \\
& - 2Q(1-v_{,2})\, v_{,12} + 2LT v_{,22} - 2R(1-v_{,2})\, v_{,22}\} - v_{,12}
\end{aligned}
$$

$$
\begin{aligned}
A_2 = \; & C[W v_{,22} + 2T v_{,12} + 2Y u_{,2} + 2U(1-u_{,1}) + X v_{,11} + 3L^4 v_{,11} - 12 L^3 M v_{,1}] \\
& + L\,\{-2L(1-u_{,1})(u_{,11} + u_{,22})\, v_{,1} - 2L^2 u_{,12} - 2N v_{,1} u_{,12} - 2S u_{,11} v_{,1} - 2Z v_{,1} u_{,22} \\
& + L[W + 2(v_{,1})^2]\, v_{,11} - 2P v_{,1} v_{,11} - 2LT v_{,12} - 2Q v_{,12} v_{,1} + L[(v_{,1})^2 \\
& - (1-u_{,1})^2]\, v_{,22} - 2R v_{,1} v_{,22}\} + v_{,11}
\end{aligned}
$$

$$A_{11} = C[X(1-v_{,2}) + 3L^4(1-v_{,2})] + L^2 S + (1-v_{,2})$$

$$A_{12} = C[2T(1-v_{,2}) + 3L^4 v_{,1}] + L^2 N + v_{,1}$$

$$A_{22} = C\,W\,(1 - v_{,2}) + L^2\,Z$$

$$\begin{aligned} B_1 = {} & C\,[2\,V\,v_{,1} + 2\,U\,(1 - v_{,2}) + 3\,L^4\,u_{,12} - 12\,L^3\,M\,u_{,2}] \\ & + L\,\{2L\,[(1 - v_{,2})\,v_{,1} - (1 - u_{,1})\,u_{,2}]\,u_{,11} - 2\,S\,u_{,11}\,u_{,2} \\ & + L\,[(1 - u_{,1})^2 + (u_{,2})^2 + 3\,(v_{,1})^2 - (1 - v_{,2})^2]\,u_{,12} - 2LT\,u_{,22} - 2Z\,u_{,22}\,u_{,2} \\ & + 2L\,[3\,v_{,1}\,u_{,2} - (1 - u_{,1})(1 - v_{,2})]\,v_{,11} - 2\,P\,v_{,11}\,u_{,2} - 2N\,u_{,12}\,u_{,2} \\ & + 2L\,[(1 - u_{,1})\,v_{,1} - (1 - v_{,2})\,u_{,2}]\,v_{,12} - 2Q\,u_{,2}\,v_{,12} - 2L^2\,v_{,22} - 2R\,u_{,2}\,v_{,22}\} \\ & + u_{,12} \end{aligned}$$

$$\begin{aligned} B_2 = {} & -C\,[W\,u_{,22} + 2T\,u_{,12} + X\,u_{,11} + 2Y\,(1 - v_{,2}) + 3L^4\,u_{,11} + 2U\,v_{,1} + 12\,L^3\,M\,(1 - u_{,1})] \\ & + L\,\{-L\,[3\,(1 - u_{,1})^2 + (v_{,1})^2]\,u_{,11} - 2S\,(1 - u_{,1})\,u_{,11} + 2LT\,u_{,12} - 2N\,(1 - u_{,1})\,u_{,12} \\ & + L\,[(v_{,1})^2 - (1 - u_{,1})^2]\,u_{,22} - 2Z\,(1 - u_{,1})\,u_{,22} + 2L\,(1 - u_{,1})\,v_{,1}\,(v_{,11} + v_{,22}) \\ & - 2\,P\,(1 - u_{,1})\,v_{,11} - 2L^2\,v_{,12} - 2Q\,(1 - u_{,1})\,v_{,12} \\ & - 2R\,(1 - u_{,1})\,v_{,22}\} - u_{,11} \end{aligned}$$

$$B_{11} = C\,[X\,u_{,2} + 3\,L^4\,u_{,2}] + L^2\,P + u_{,2}$$

$$B_{12} = C\,[2T\,u_{,2} + 3L^4\,(1 - u_{,1})] + L^2\,Q + (1 - u_{,1})$$

$$B_{22} = C\,W\,u_{,2} + L^2\,R$$

$$\begin{aligned} K_1 = {} & C\,[W\,V + 2\,T\,U + XY + 3\,L^4\,M] \\ & + L^2\,[S\,u_{,11} + N\,u_{,12} + Z\,u_{,22} + P\,v_{,11} + Q\,v_{,12} + R\,v_{,22}] + M \end{aligned} \qquad (A\text{-}1)$$

where

$$C = C_1/C_2$$

$$L = (1 - u_{,1})(1 - v_{,2}) - u_{,2}\, v_{,1}$$

$$M = (1 - v_{,2})\, u_{,11} + (1 - u_{,1})\, v_{,12} + u_{,21}\, v_{,1} + u_{,2}\, v_{,11}$$

$$N = (1 - u_{,1})^2\, v_{,1} + (v_{,1})^3 - 2u_{,2}(1 - u_{,1})(1 - v_{,2}) - v_{,1}(1 - v_{,2})^2 + (u_{,2})^2\, v_{,1}$$

$$P = u_{,2}(1 - u_{,1})^2 - 2v_{,1}(1 - u_{,1})(1 - v_{,2}) + 3u_{,2}(v_{,1})^2$$

$$Q = (1 - u_{,1})^3 + (1 - u_{,1})[(v_{,1})^2 - (u_{,2})^2] - 2u_{,2}v_{,1}(1 - v_{,2}) + (1 - v_{,2})^2(1 - u_{,1})$$

$$R = u_{,2}(v_{,1})^2 - u_{,2}(1 - u_{,1})^2 - 2v_{,1}(1 - u_{,1})(1 - v_{,2})$$

$$S = (1 - v_{,2})(v_{,1})^2 + 3(1 - u_{,1})^2(1 - v_{,2}) - 2(1 - u_{,1})\, u_{,2}\, v_{,1}$$

$$T = u_{,2}(1 - u_{,1}) + v_{,1}(1 - v_{,2})$$

$$U = (1 - v_{,2})\, u_{,12} + u_{,2}\, v_{,12}$$

$$V = (1 - v_{,2})\, u_{,22} + u_{,2}\, v_{,22}$$

$$W = (1 - u_{,1})^2 + (v_{,1})^2$$

$$X = (1 - v_{,2})^2 + (u_{,2})^2$$

$$Y = (1 - v_{,2})\, u_{,11} + u_{,2}\, v_{,11}$$

$$Z = (1 - u_{,1})^2(1 - v_{,2}) - 2u_{,2}\, v_{,1}(1 - u_{,1}) - (v_{,1})^2(1 - v_{,2}) \qquad \text{(A-2)}$$

and

$$D_1 = -C[\bar{W}v_{,11} + 2\bar{T}v_{,12} + 2\bar{U}u_{,2} + \bar{X}v_{,22} + 3\bar{L}^4 v_{,22} + 12\bar{L}^3\bar{M}(1 - v_{,2})$$

$$+ 2\bar{Y}(1 - u_{,1})] + \bar{L}\{2\bar{L}(1 - v_{,2})u_{,2}(u_{,11} + u_{,22}) - 2\bar{R}(1 - v_{,2})u_{,11} - 2\bar{L}^2 u_{,12}$$

$$- 2\bar{Q}(1 - v_{,2})u_{,12} - 2\bar{P}(1 - v_{,2})u_{,22} + \bar{L}[(u_{,2})^2 - (1 - v_{,2})^2]v_{,11}$$

$$- 2\bar{Z}(1 - v_{,2})\, v_{,11} + 2\bar{L}\bar{T}\, v_{,12} - 2\bar{N}(1 - v_{,2})\, v_{,12} - \bar{L}[(u_{,2})^2 + 3(1 - v_{,2})^2]\, v_{,22}$$
$$- 2\bar{S}(1 - v_{,2})\, v_{,22} \} - v_{,22}$$

$$D_2 = C[2\bar{V} u_{,2} + 2\bar{U}(1 - u_{,1}) + 3\bar{L}^4 v_{,12} - 12\bar{L}^3 \bar{M} v_{,1}]$$
$$+ \bar{L}\{-2\bar{L}^2 u_{,11} - 2\bar{R} v_{,1} u_{,11} + 2\bar{L}[(1 - v_{,2})\, u_{,2} - (1 - u_{,1})\, v_{,1}]\, u_{,12}$$
$$- 2\bar{Q} v_{,1} u_{,12} + 2\bar{L}[3 u_{,2} v_{,1} - (1 - u_{,1})(1 - v_{,2})]\, u_{,22} - 2\bar{P} u_{,22} v_{,1}$$
$$- 2\bar{L}\bar{T} v_{,11} - 2\bar{Z} v_{,11} v_{,1} + \bar{L}[(1 - v_{,2})^2 + 3(u_{,2})^2 + (v_{,1})^2 - (1 - u_{,1})^2]\, v_{,12}$$
$$- 2\bar{N} v_{,1} v_{,12} + 2\bar{L}[u_{,2}(1 - u_{,1}) - v_{,1}(1 - v_{,2})]\, v_{,22} - 2\bar{S} v_{,22} v_{,1}\}$$
$$+ v_{,12}$$

$$D_{11} = C\bar{W} v_{,1} + \bar{L}^2 \bar{R}$$

$$D_{12} = C[2\bar{T} v_{,1} + 3\bar{L}^4 (1 - v_{,2})] + \bar{L}^2 \bar{Q} + 1 - v_{,2}$$

$$D_{22} = C[\bar{X} v_{,1} + 3\bar{L}^4 v_{,1}] + \bar{L}^2 \bar{P} + v_{,1}$$

$$E_1 = C[\bar{W} u_{,11} + 2\bar{T} u_{,12} + \bar{X} u_{,22} + 2\bar{Y} v_{,1} + 3\bar{L}^4 u_{,22} - 12\bar{L}^3 \bar{M} u_{,2}$$
$$+ 2\bar{U}(1 - v_{,2})]$$
$$+ \bar{L}\{-\bar{L}[(1 - v_{,2})^2 - (u_{,2})^2]\, u_{,11} - 2\bar{R} u_{,11} u_{,2} - 2\bar{L}\bar{T} u_{,12}$$
$$- 2\bar{Q} u_{,12} u_{,2} + \bar{L}[(1 - v_{,2})^2 + 3(u_{,2})^2]\, u_{,22} - 2\bar{P} u_{,22} u_{,2}$$
$$- 2\bar{L}(1 - v_{,2})\, u_{,2} (v_{,11} + v_{,22}) - 2\bar{Z} v_{,11} u_{,2} - 2\bar{L}^2 v_{,12} - 2\bar{N} v_{,12} u_{,2}$$
$$- 2\bar{S} v_{,22} u_{,2}\} + u_{,22}$$

$$E_2 = C\,[-2\bar{V}\,(1 - v,_2) - 2\,\bar{U}\,v,_1 - 3\,\bar{L}^4\,u,_{12} - 12\,\bar{L}^3\,\bar{M}(1 - u,_1)]$$

$$+ \bar{L}\{2\bar{L}\bar{T}\,u,_{11} - 2\,\bar{R}(1 - u,_1)\,u,_{11} + \bar{L}\,[(v,_1)^2 - (u,_2)^2 - 3(1-v,_2)^2$$

$$-(1-u,_1)^2]\,u,_{12} - 2\bar{Q}\,(1-u,_1)\,u,_{12} + 2\bar{L}[(1-u,_1)\,u,_2 - (1-v,_2)\,v,_1]\,u,_{22}$$

$$- 2\bar{P}\,(1-u,_1)\,u,_{22} - 2\bar{L}^2\,v,_{11} - 2\bar{Z}(1-u,_1)\,(v,_{11}) + 2\bar{L}\,[(1-u,_1)\,v,_1$$

$$- (1-v,_2)u,_2]v,_{12} - 2\bar{N}\,(1-u,_1)v,_{12} + 2\bar{L}[u,_2\,v,_1 - 3\,(1-u,_1)(1-v,_2)]v,_{22}$$

$$- 2\bar{S}\,(1-u,_1)\,v,_{22}\} - u,_{12}$$

$$E_{11} = C\,\bar{W}\,(1 - u,_1) + \bar{L}^2\,\bar{Z}$$

$$E_{12} = C\,[2\bar{T}\,(1 - u,_1) + 3\bar{L}^4\,u,_2] + \bar{L}^2\,\bar{N} + u,_2$$

$$E_{22} = C\,[\bar{X}\,(1-u,_1) + 3\bar{L}^4\,(1 - u,_1)] + \bar{L}^2\,\bar{S} + 1 - u,_1$$

$$K_2 = C\,[\bar{W}\,\bar{V} + 2\,\bar{T}\,\bar{U} + \bar{X}\bar{Y} + 3\,\bar{L}^4\,\bar{M}]$$

$$+ L^2\,[\bar{R}u,_{11} + \bar{Q}u,_{12} + \bar{P}u,_{22} + \bar{Z}\,v,_{11} + \bar{N}\,v,_{12} + \bar{S}v,_{22}] + \bar{M} \qquad \text{(A-3)}$$

where

$$\bar{L} = (1-u,_1)(1-v,_2) - u,_2\,v,_1$$

$$\bar{M} = (1-u,_1)\,v,_{22} + (1-v,_2)\,u,_{12} + v,_{12}u,_2 + v,_1\,u,_{22}$$

$$\bar{N} = (1-v,_2)^2\,u,_2 + (u,_2)^3 - 2\,(1-u,_1)\,(1-v,_2)\,v,_1 - (1-u,_1)^2u,_2 + (v,_1)^2u,_2$$

$$\bar{P} = v,_1\,(1-v,_2)^2 - 2\,u,_2\,(1-u,_1)\,(1-v,_2) + 3\,(u,_2)^2\,v,_1$$

$$\bar{Q} = (1-v,_2)^3 + (1-v,_2)\,[(u,_2)^2 - (v,_1)^2] - 2u,_2v,_1\,(1-u,_1) + (1-u,_1)^2(1-v,_2)$$

$$\bar{R} = [(u,_2)^2 - (1-v,_2)^2]\,v,_1 - 2\,u,_2\,(1-u,_1)\,(1-v,_2)$$

$$\bar{S} = (1-u,_1)\,(u,_2)^2 + 3\,(1-v,_2)^2\,(1-u,_1) - 2\,(1-v,_2)\,u,_2v,_1$$

$$\bar{T} = v_{,1}(1-v_{,2}) + u_{,2}(1-u_{,1})$$

$$\bar{U} = (1-u_{,1})\, v_{,12} + v_{,1}\, u_{,12}$$

$$\bar{V} = (1-u_{,1})\, v_{,11} + v_{,1}\, u_{,11}$$

$$\bar{W} = (1-v_{,2})^2 + (u_{,2})^2$$

$$\bar{X} = (1-u_{,1})^2 + (v_{,1})^2$$

$$\bar{Y} = (1-u_{,1})\, v_{,22} + v_{,1}\, u_{,22}$$

$$\bar{Z} = (1-v_{,2})^2 (1-u_{,1}) - 2u_{,2}\, v_{,1}(1-v_{,2}) - (u_{,2})^2 (1-u_{,1}) \qquad \text{(A-4)}$$

ii) Coefficients of Linearized Stress-Displacement Equations (2-58).

$$a_1 = 4\{2C_1L^3(1-v_{,2}) + C_2L\,[W(1-v_{,2}) + L(1-u_{,1})]\}$$

$$a_2 = 4[C_1(2v_{,1}L^3 + u_{,2}) + C_2L\,W\,v_{,1}]$$

$$b_1 = 4[2C_1\,L^3u_{,2} + C_2L\,(W\,u_{,2} - v_{,1}L)]$$

$$b_2 = 4\{C_1[2L^3\,(1-u_{,1}) - (1-v_{,2})] + C_2L\,W\,(1-u_{,1})\}$$

$$k_1 = 2[C_1(X-L^4) + C_2(1-L^2\,W)]$$

$$d_1 = 4\{C_1[2L^3(1-v_{,2}) - (1-u_{,1})] + C_2L\,X\,(1-v_{,2})\}$$

$$d_2 = 4[2C_1L^3\,v_{,1} + C_2L\,(Xv_{,1} - Lu_{,2})]$$

$$e_1 = 4[C_1(2L^3u_{,2} + v_{,1}) + C_2L\,X\,u_{,2}]$$

$$e_2 = 4\{2C_1\,L^3(1-u_{,1}) + C_2L\,[X\,(1-u_{,1}) + (1-v_{,2})\,L]\}$$

$$k_2 = 2[C_1\,(W-L^4) + C_2(1 - L^2\,X)]$$

$$f_1 = -2\{C_1\,u_{,2} + C_2L\,[L\,u_{,2} + 2\,T\,(1-v_{,2})]\}$$

$$f_2 = 2\{C_1(1-u_{,1}) + C_2\,L\,[L(1-u_{,1}) - 2\,T\,v_{,1}]\}$$

$$g_1 = 2\{C_1(1-v_{,2}) + C_2\,L\,[L(1-v_{,2}) - 2\,T\,u_{,2}]\}$$

$$g_2 = -2\{C_1\,v_{,1} + C_2\,L\,[L\,v_{,1} + 2\,T\,(1-u_{,1})]\}$$

$$k_3 = 2\,T\,[C_1 + C_2\,L^2] \qquad \text{(A-5)}$$

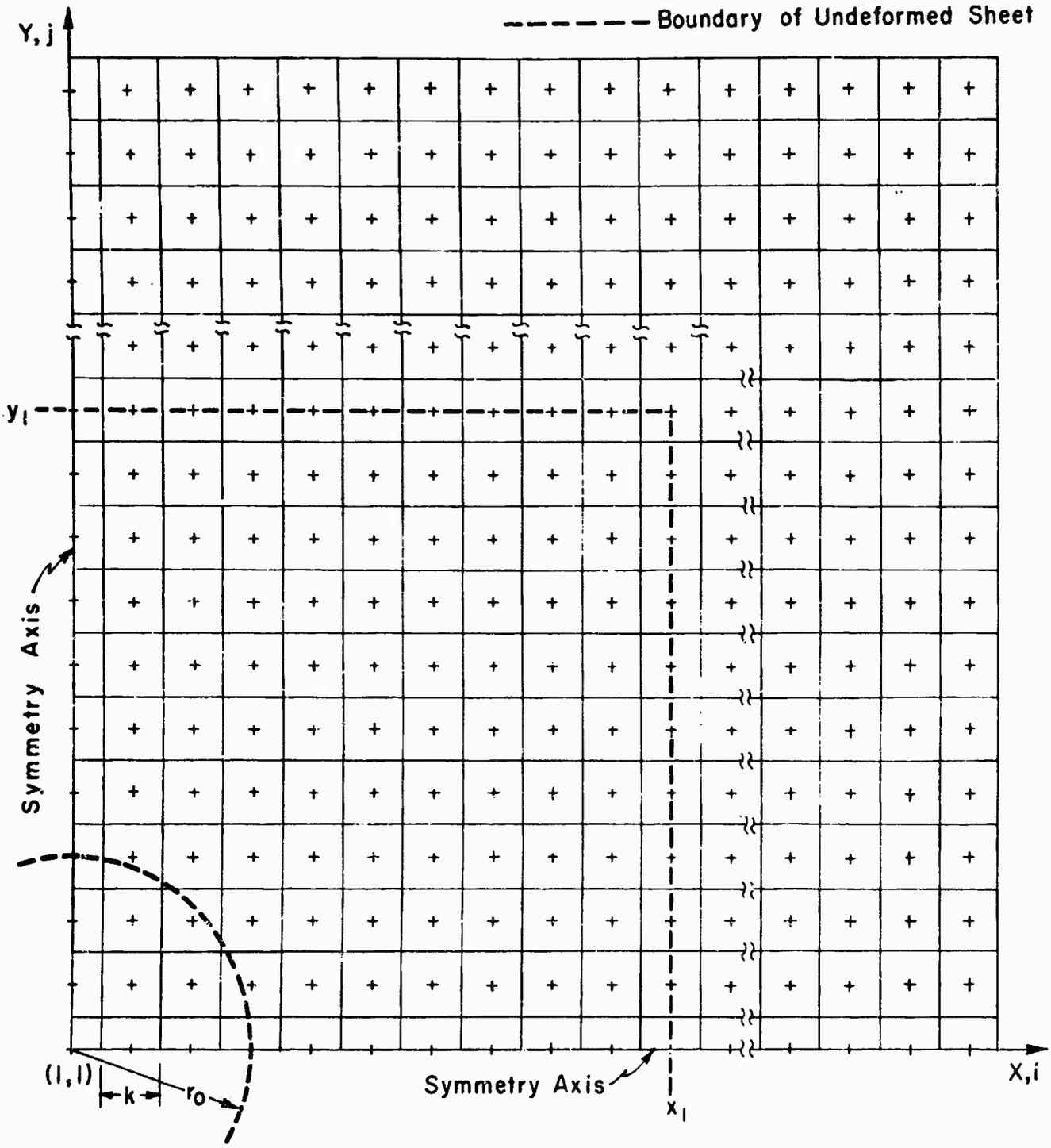

FIG. 1 EULERIAN GRID

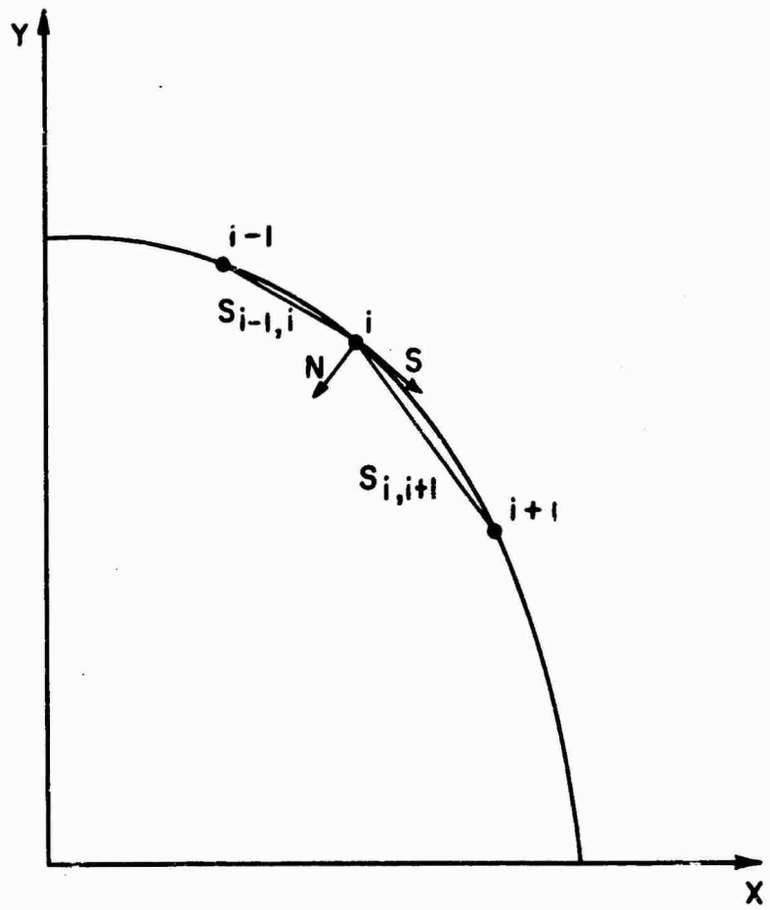

FIG. 2 BOUNDARY POINTS AT EDGE OF HOLE

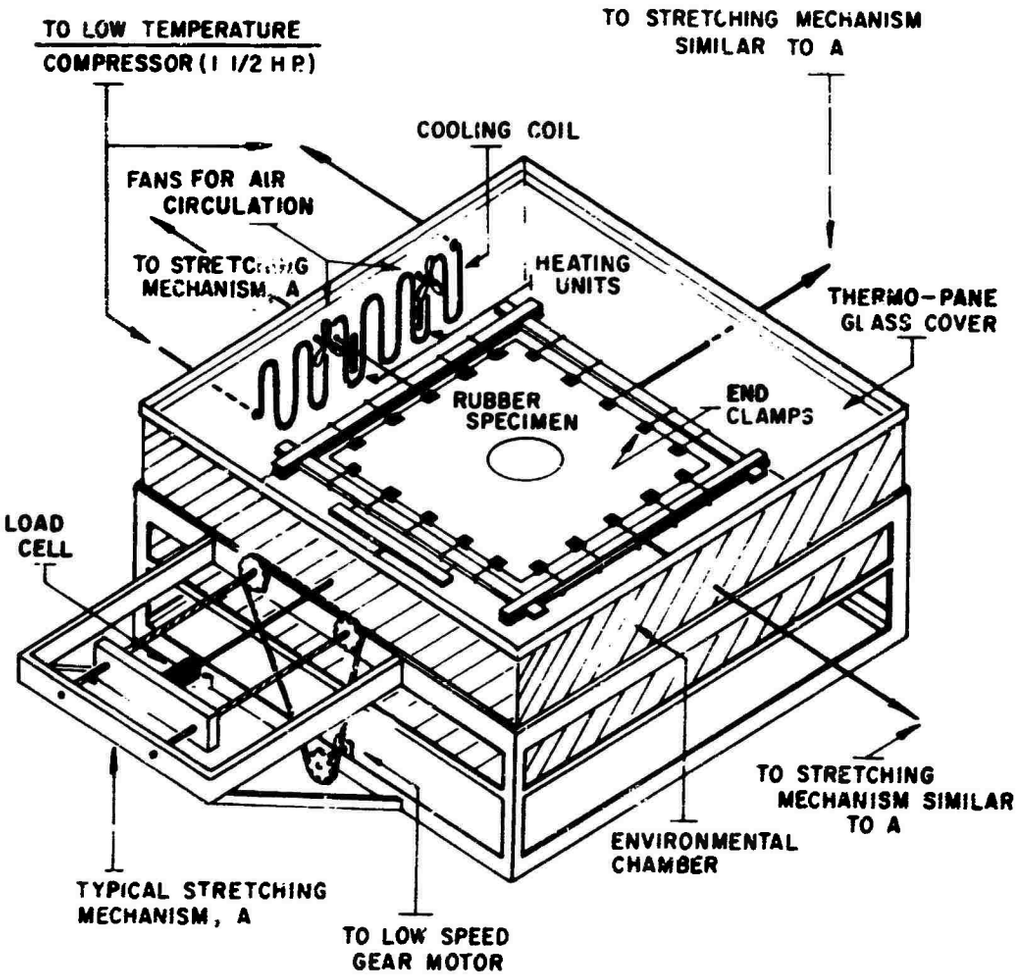

FIG. 3 · BIAXIAL TESTING APPARATUS

FIG. 4 PHOTOGRAPH OF SPECIMEN IN LOADING FRAME

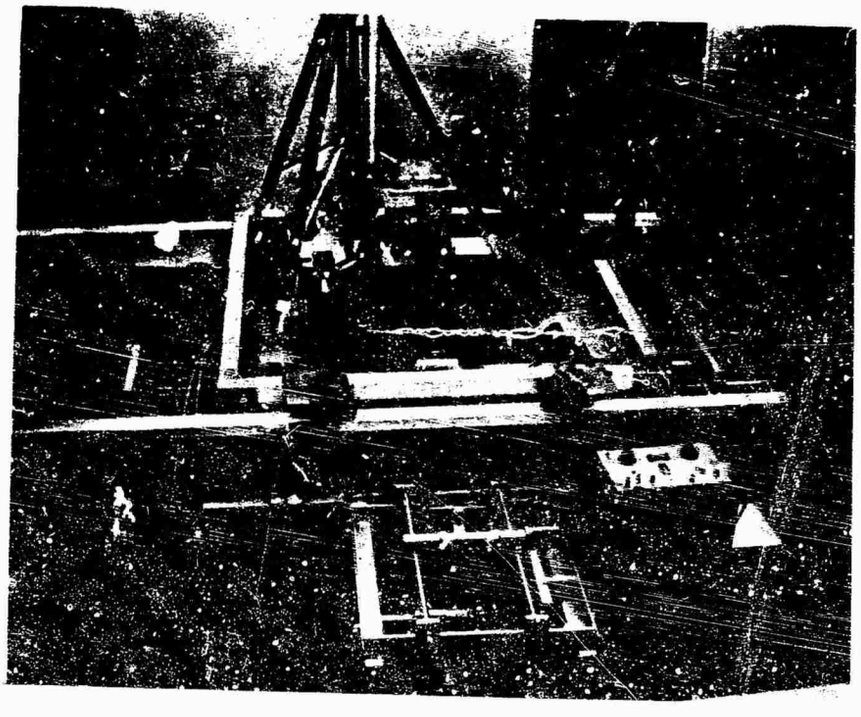

FIG. 5 PHOTOGRAPH OF TEST SET-UP

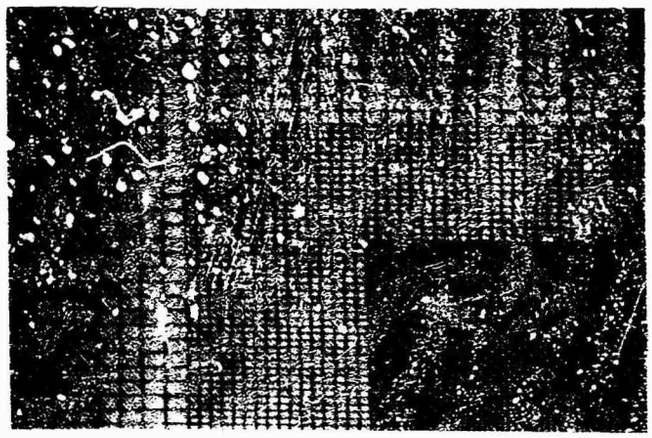

FIG. 6 PHOTOGRAPH OF ONE-QUARTER OF UNDEFORMED GRID

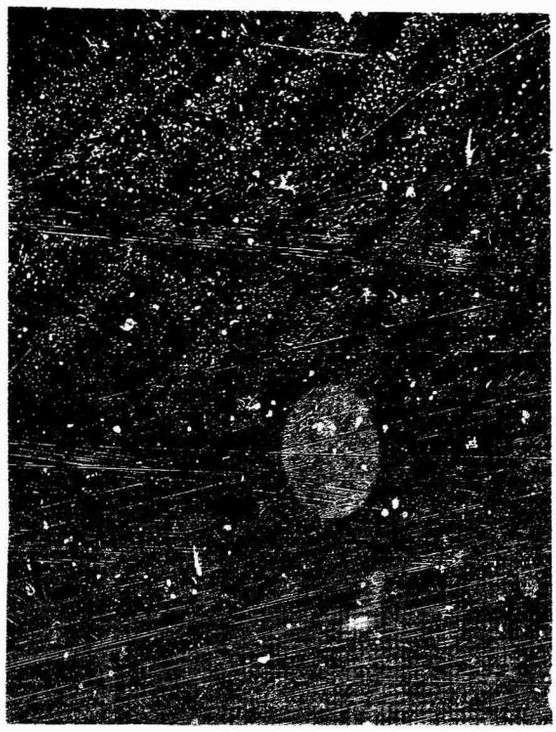

FIG. 7 PHOTOGRAPH OF DEFORMED GRID (GRID SPACING: 1/32 - 1/4 in.)

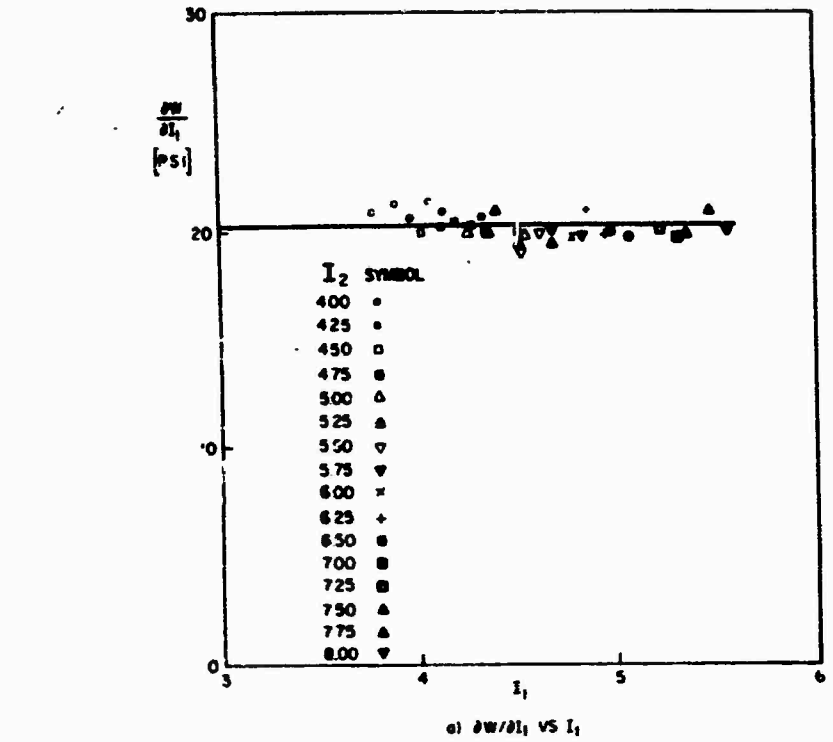

a) $\partial W/\partial I_1$ VS I_1

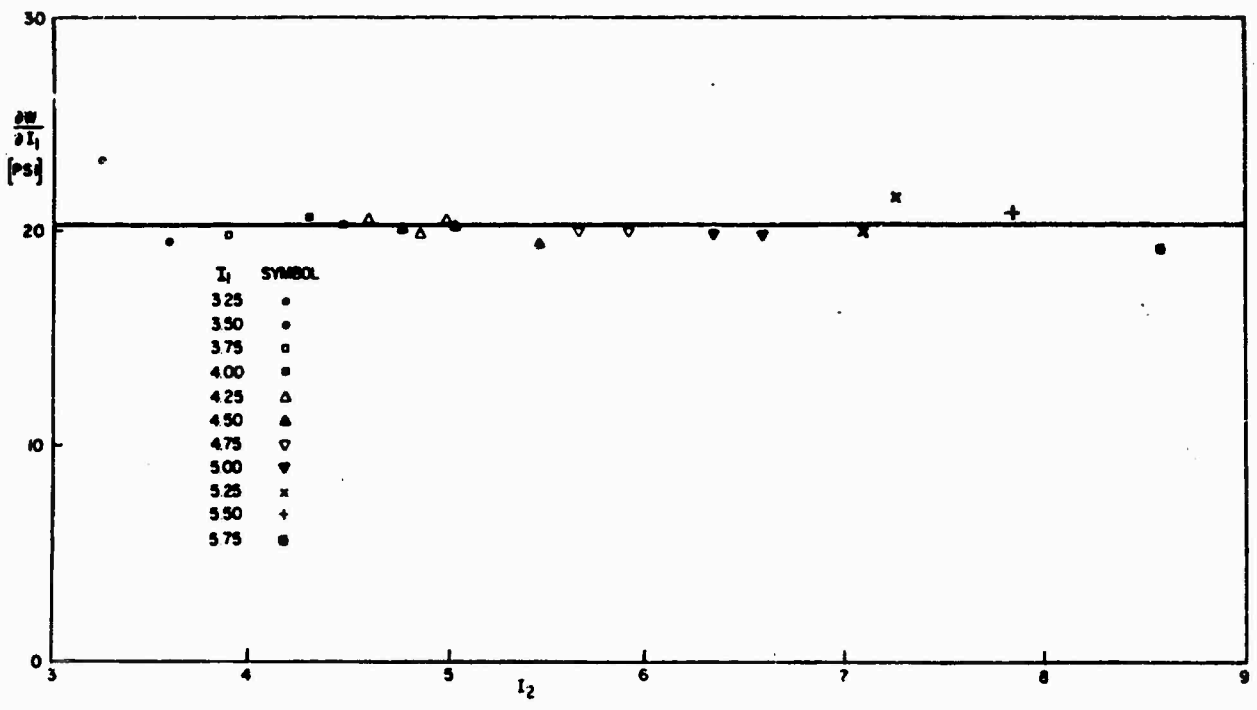

b) $\partial W/\partial I_1$ VS I_2

FIG. 8 BIAXIAL TEST: $\frac{\partial W}{\partial I_1}$ AS A FUNCTION OF I_1 AND I_2

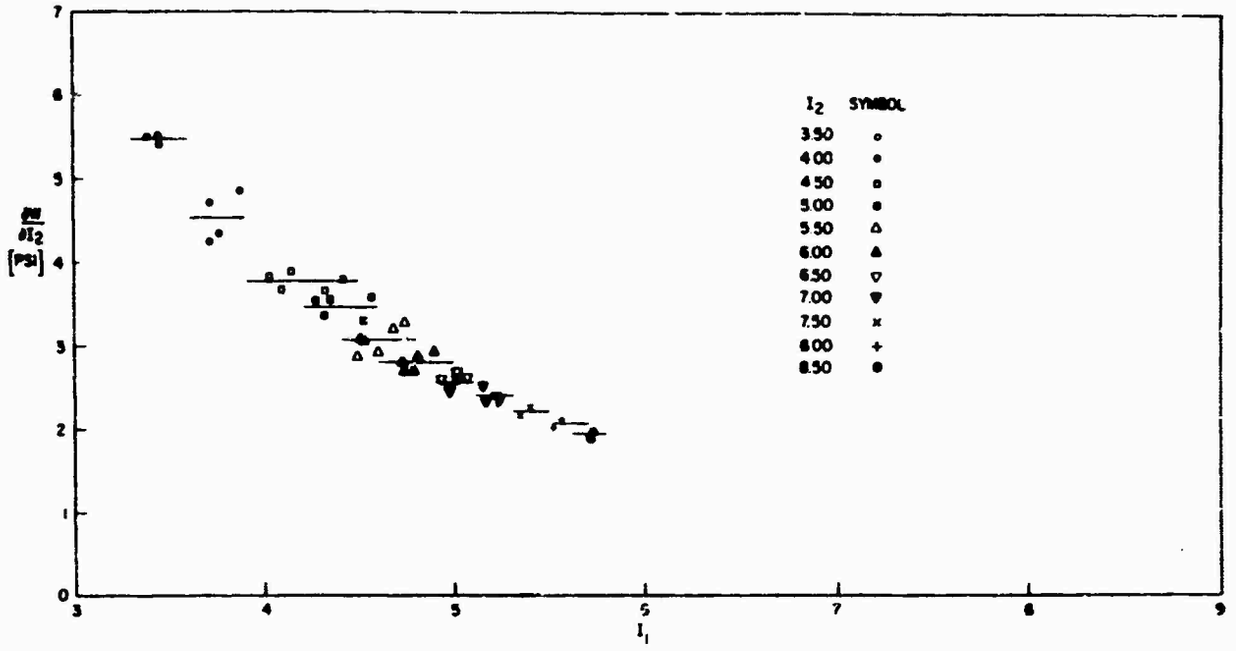

a) $\partial W/\partial I_2$ VS I_1

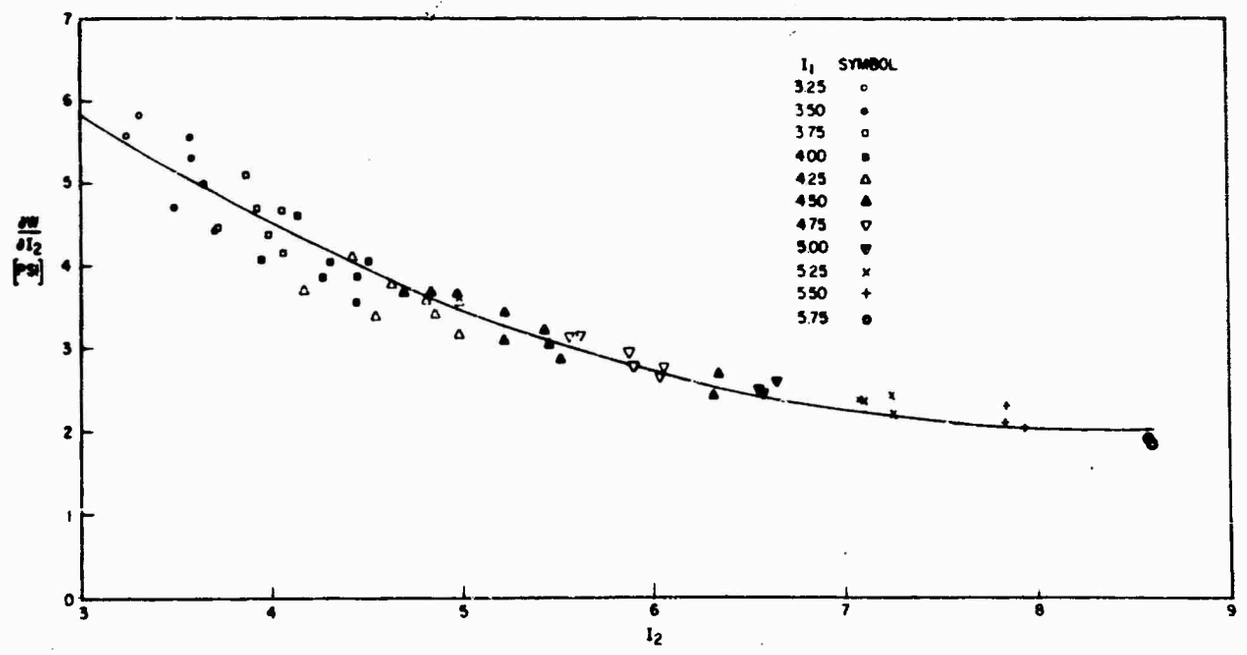

b) $\partial W/\partial I_2$ VS I_2

FIG. 9 BIAXIAL TEST: $\frac{\partial W}{\partial I_2}$ AS A FUNCTION OF I_1 AND I_2

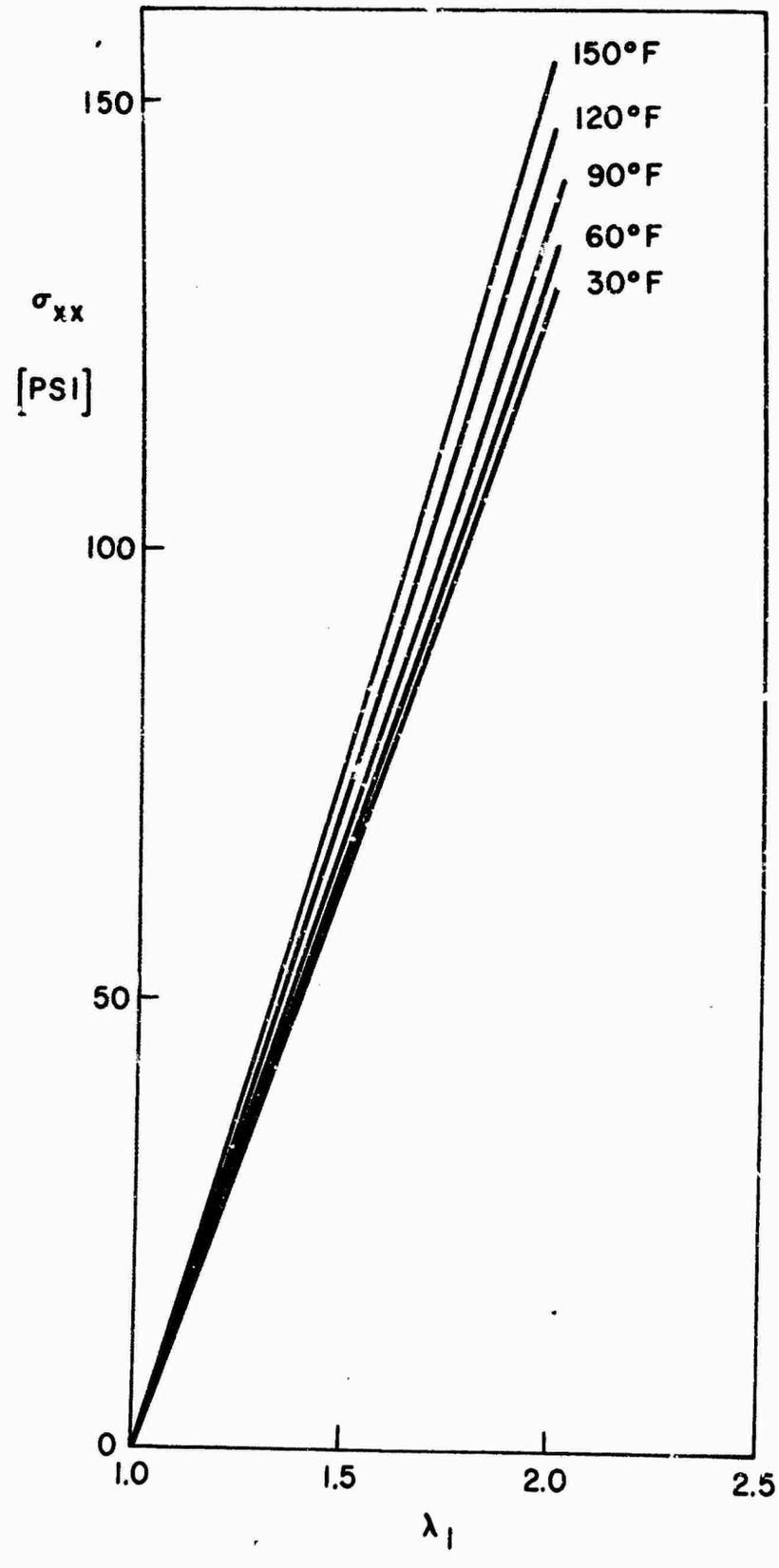

FIG. 10 TEMPERATURE DEPENDENCE OF STRIP IN UNIAXIAL TENSION

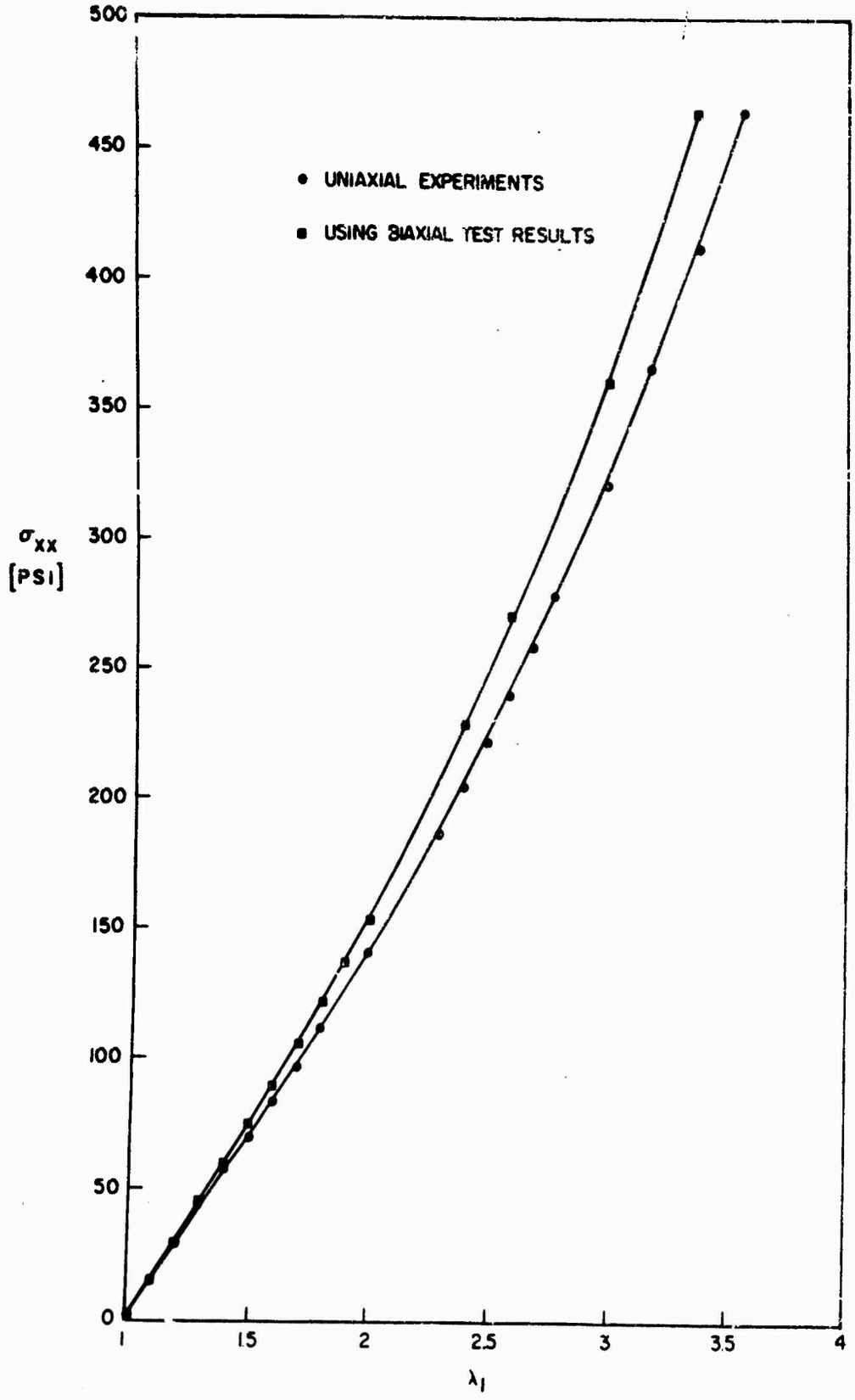

FIG. 11 UNIAXIAL TENSION OF STRIP AT 90°F

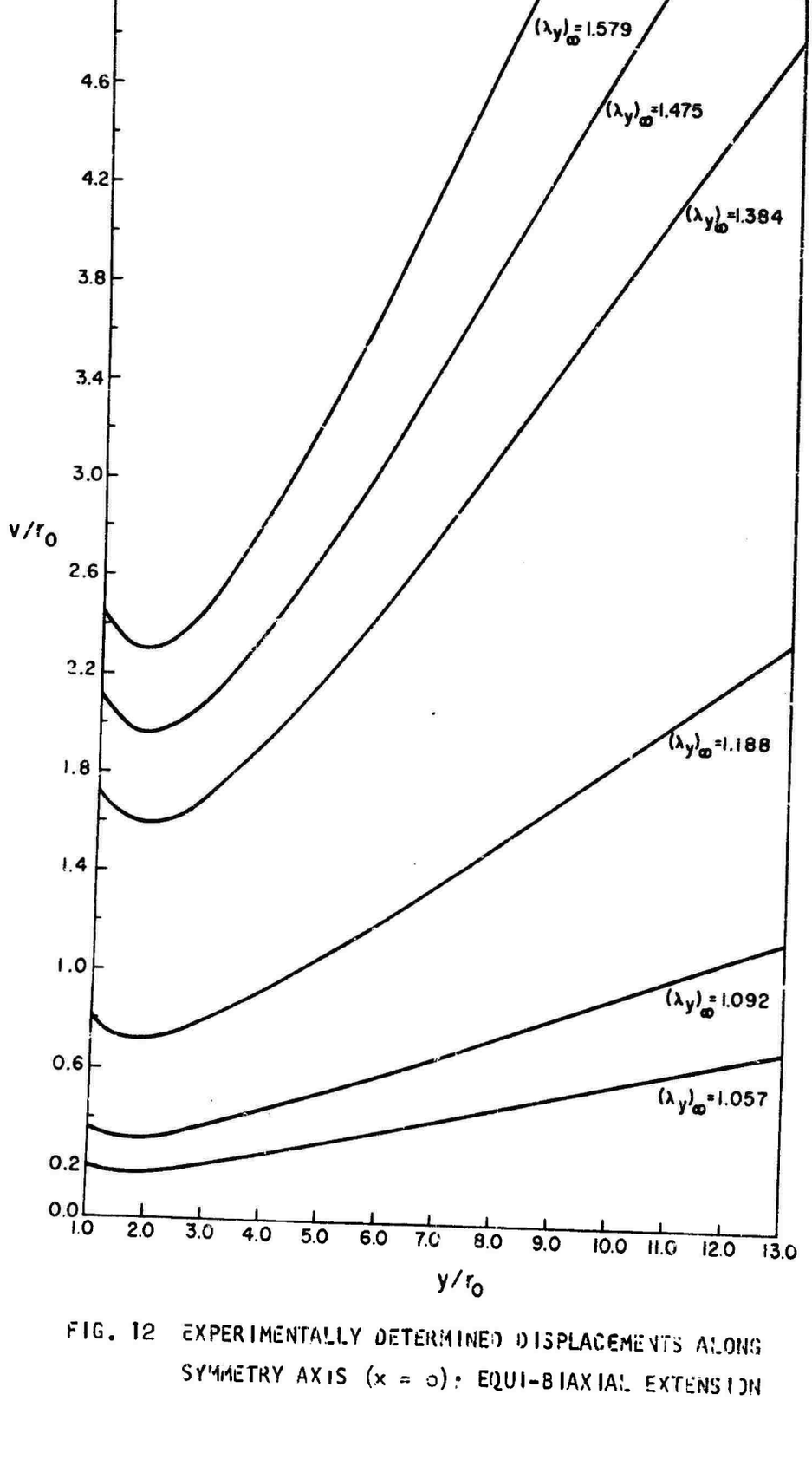

FIG. 12 EXPERIMENTALLY DETERMINED DISPLACEMENTS ALONG SYMMETRY AXIS (x = 0): EQUI-BIAXIAL EXTENSION

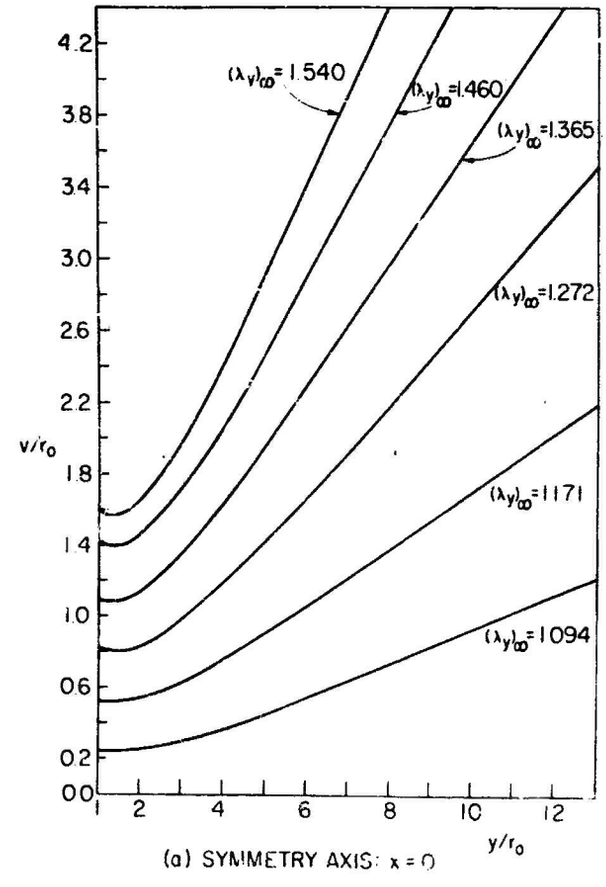

(a) SYMMETRY AXIS: x = 0

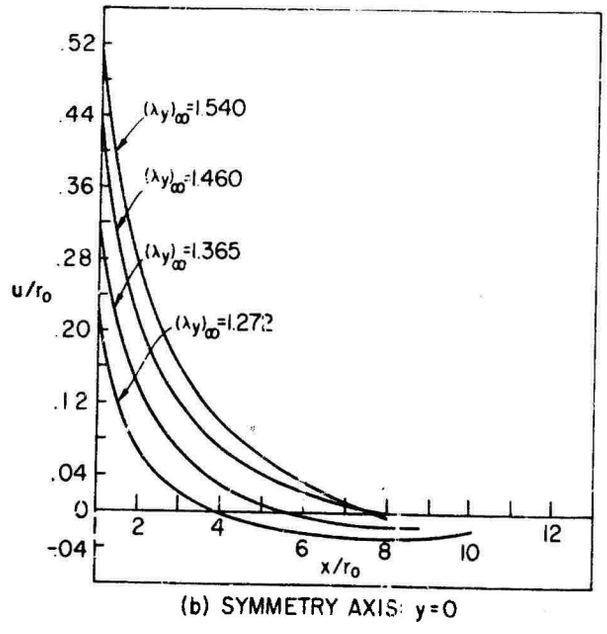

(b) SYMMETRY AXIS: y=0

FIG. 13 EXPERIMENTALLY DETERMINED DISPLACEMENTS ALONG SYMMETRY AXIS: BIAXIAL EXTENSION [$(\lambda_x)_\infty = 1.0$]

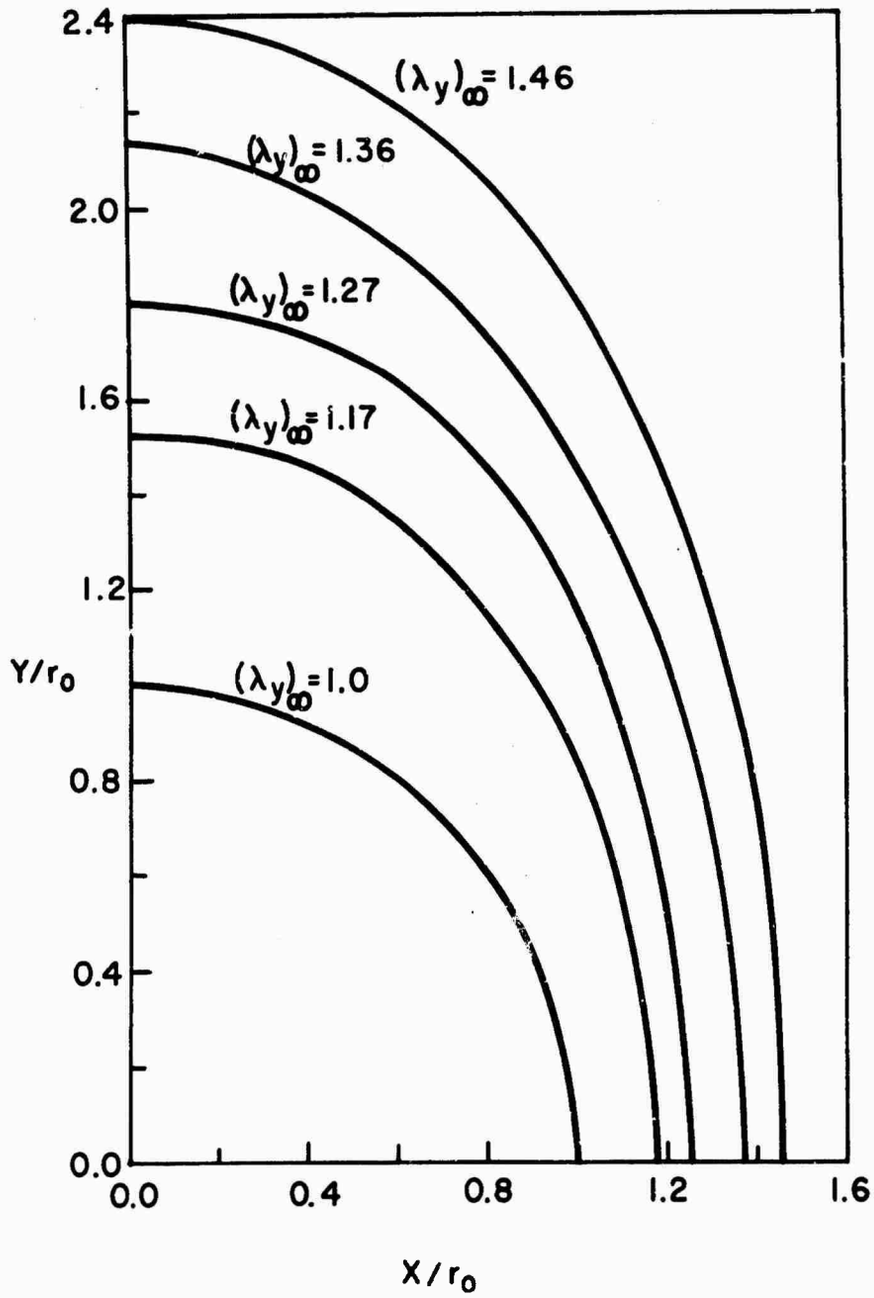

FIG. 14 SHAPE OF HOLE: BIAXIAL EXTENSION [$(\lambda_x)_\infty = 1.0$]

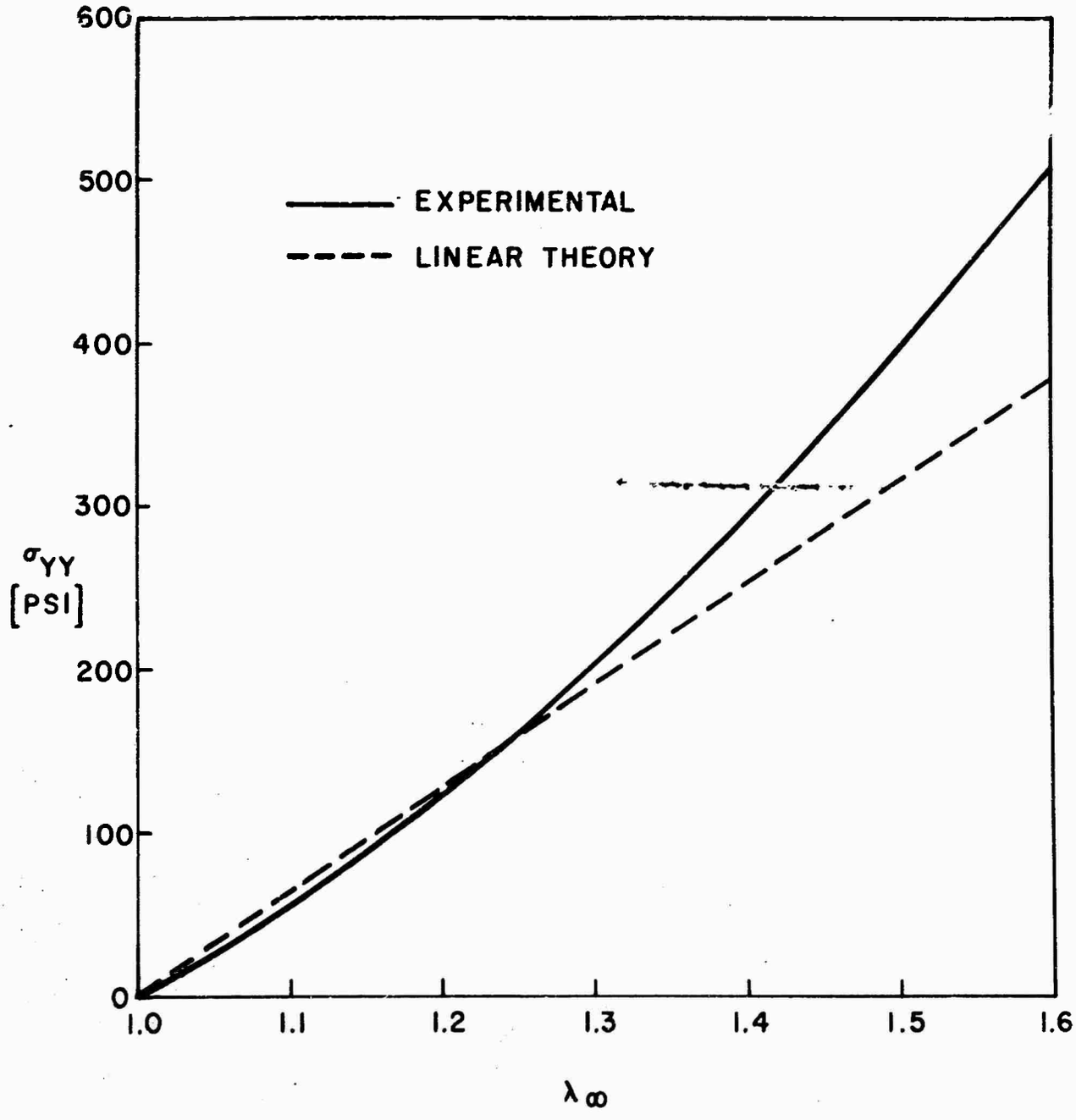

FIG. 15 (CIRCUMFERENTIAL) STRESS AT EDGE OF HOLE ($x = r_o$, $y = o$)
EQUI-BIAXIAL EXTENSION

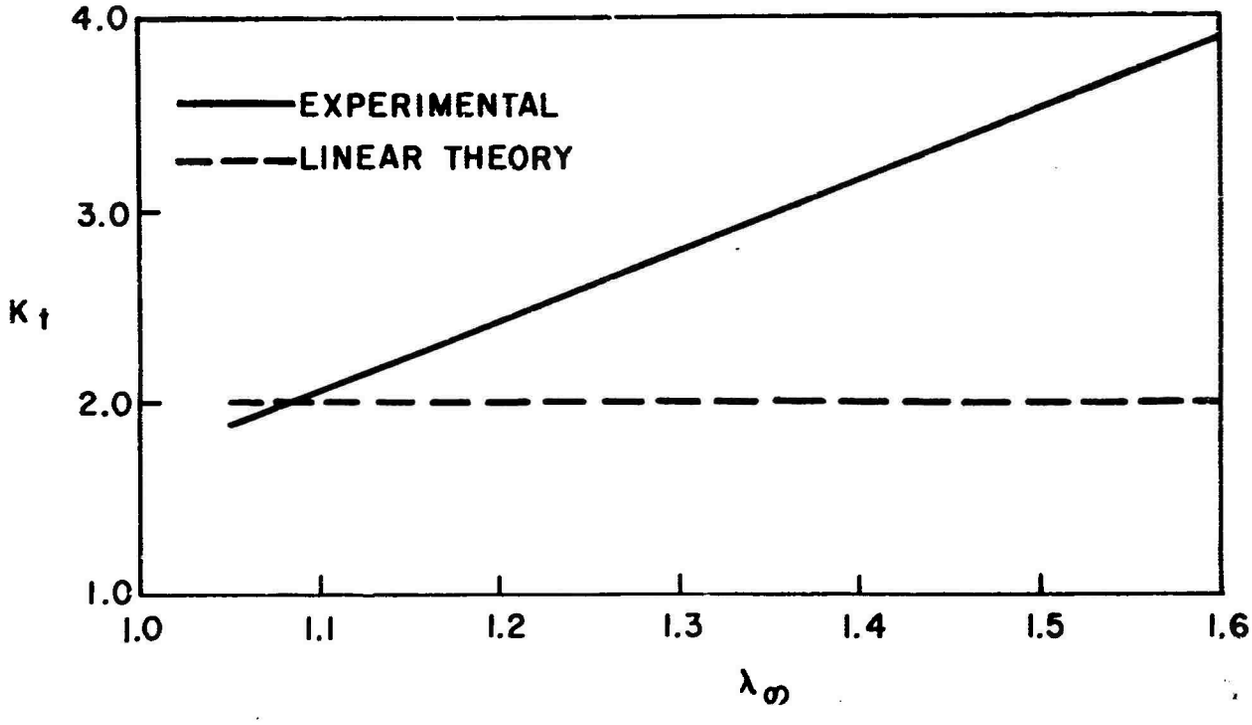

FIG. 16 STRESS CONCENTRATION FACTOR AROUND HOLE (K_t)
EQUI-BIAXIAL EXTENSION

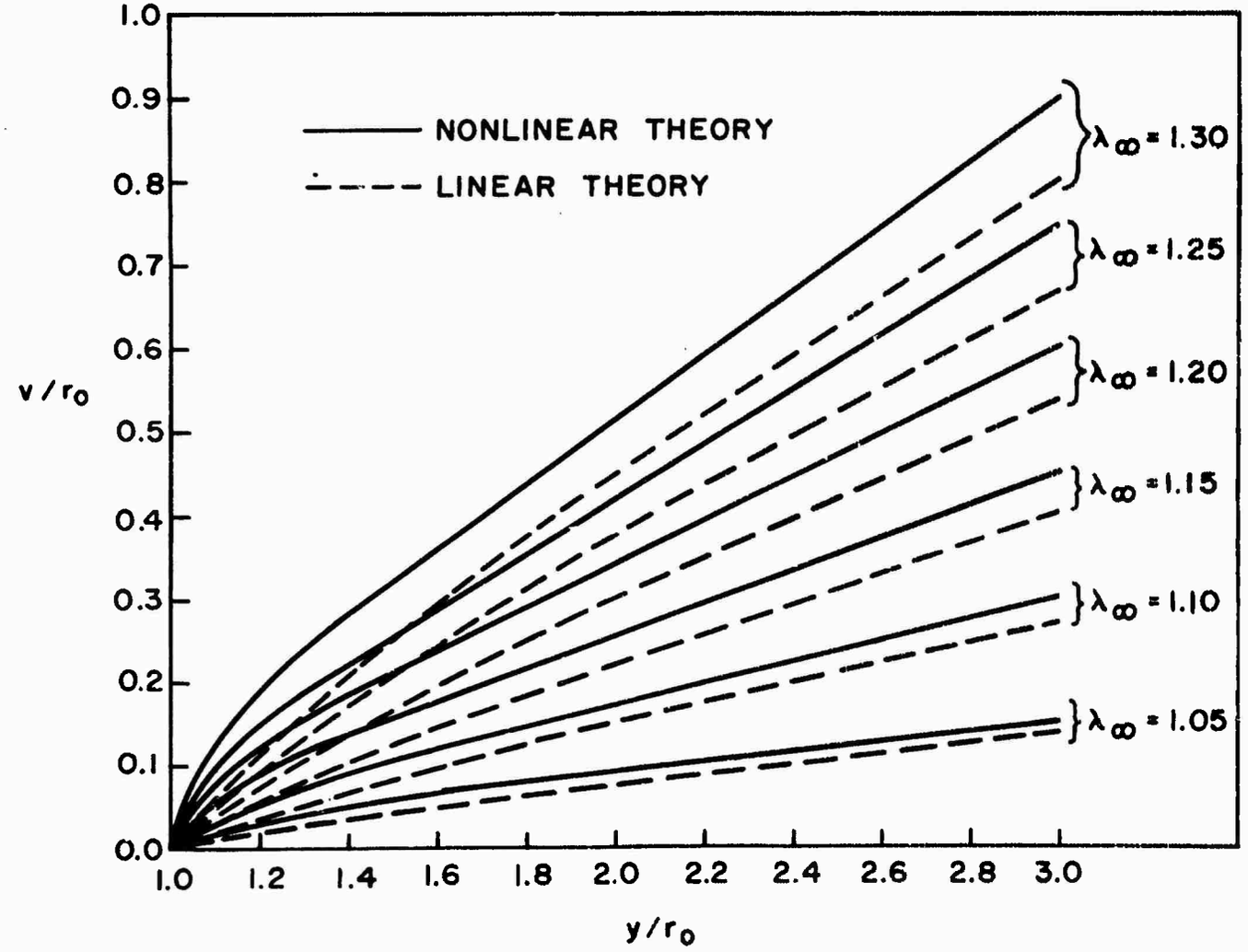

FIG. 17 DISPLACEMENT ALONG SYMMETRY AXIS (x = o)
RIGID INCLUSION, EQUI-BIAXIAL EXTENSION

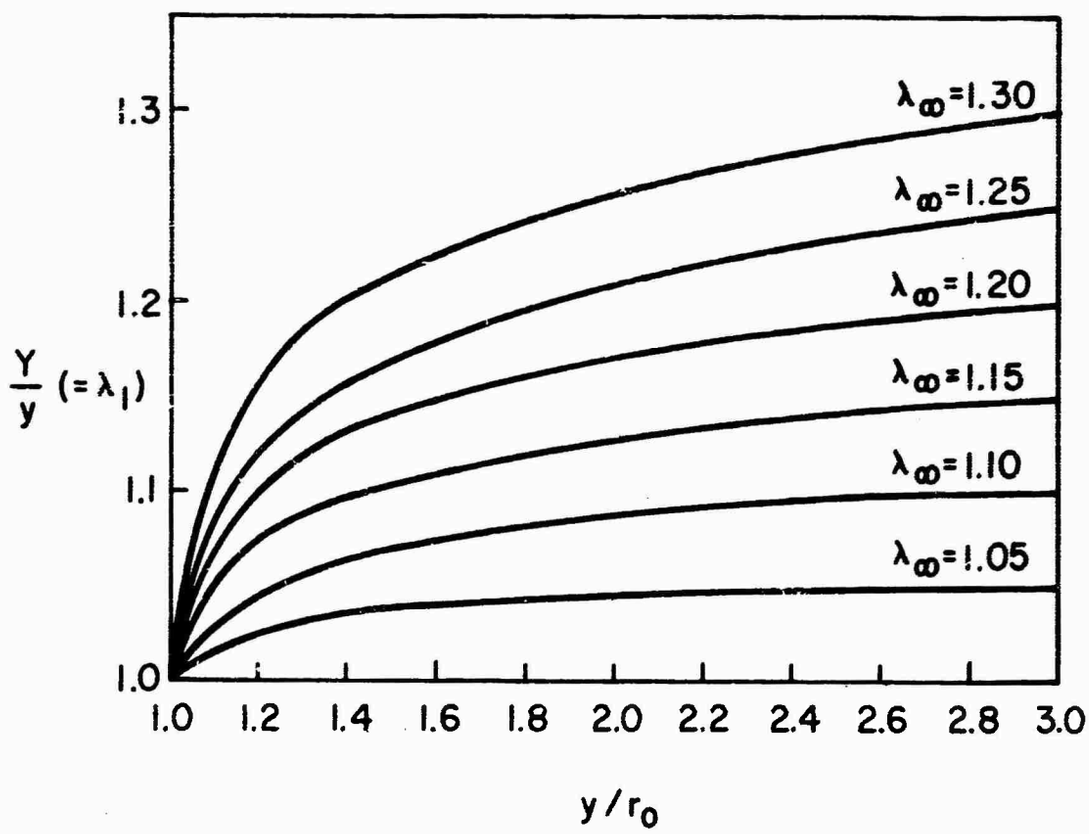

FIG. 18 (CIRCUMFERENTIAL) EXTENSION RATIO ALONG AXIS OF SYMMETRY (x = o)

RIGID INCLUSION, EQUI-BIAXIAL EXTENSION

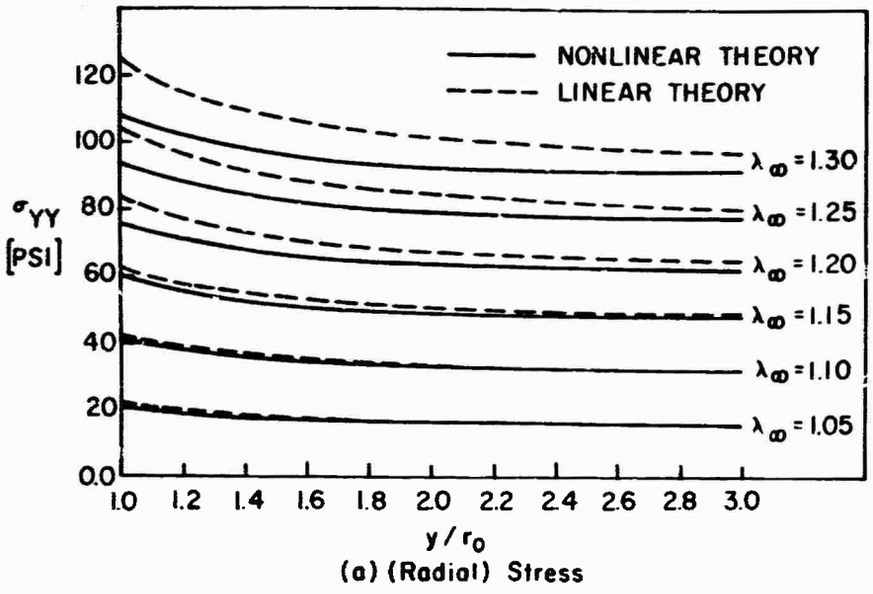

(a) (Radial) Stress

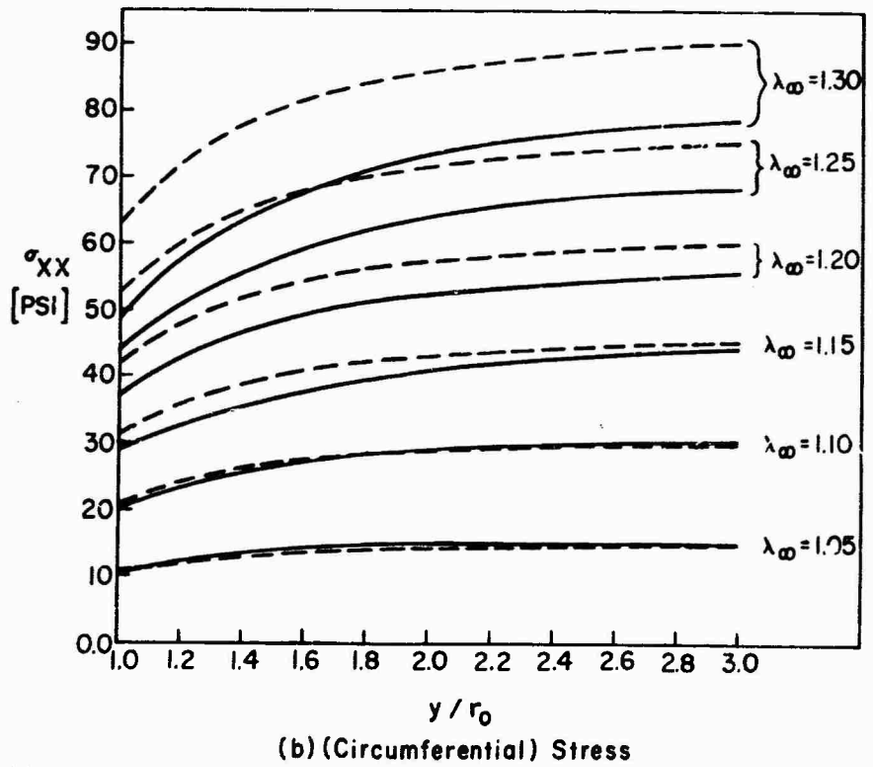

(b) (Circumferential) Stress

FIG. 19 STRESS DISTRIBUTION ALONG SYMMETRY AXIS (x = o)
RIGID INCLUSION, EQUI-BIAXIAL EXTENSION

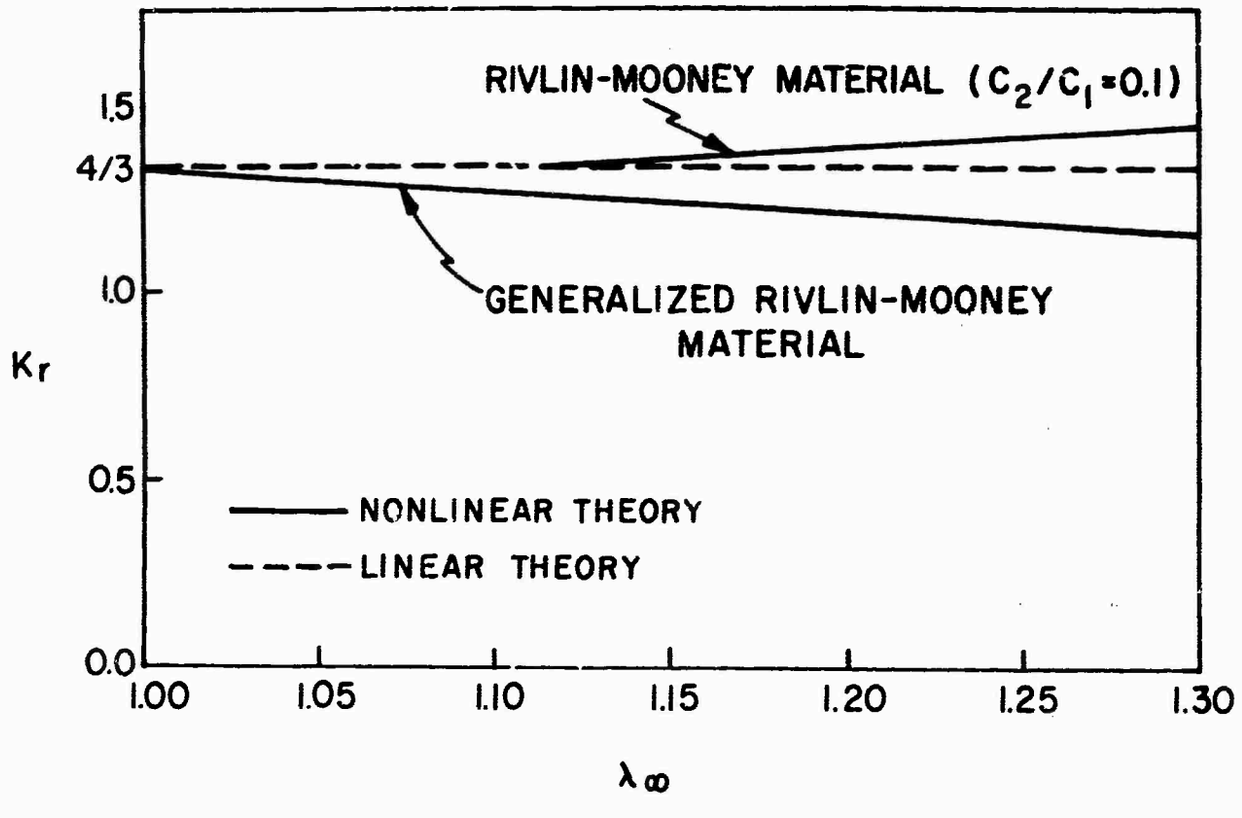

FIG. 20 STRESS CONCENTRATION FACTOR AT RIGID INCLUSION (K_r)
EQUI-BIAXIAL EXTENSION

UNCLASSIFIED

Security Classification

DOCUMENT CONTROL DATA - R & D

(Security classification of title, body of abstract and indexing annotation must be entered when the overall report is classified)

1. ORIGINATING ACTIVITY (Corporate author)	2a. REPORT SECURITY CLASSIFICATION
Polytechnic Institute of Brooklyn Dept. of Aerospace Engineering & Applied Mechanics 333 Jay St., Brooklyn, N. Y. 11201	UNCLASSIFIED 2b. GROUP

3. REPORT TITLE

STRESS CONCENTRATION IN AN ELASTOMERIC SHEET SUBJECT TO LARGE DEFORMATIONS

4. DESCRIPTIVE NOTES *(Type of report and inclusive dates)*

INTERIM TECHNICAL REPORTS

5. AUTHOR(S) *(First name, middle initial, last name)*

Alexander Segal and J. M. Klosner

6. REPORT DATE	7a. TOTAL NO. OF PAGES	7b. NO. OF REFS
MARCH 1970	73	

8a. CONTRACT OR GRANT NO.	9a. ORIGINATOR'S REPORT NUMBER(S)
DAHC04-69-C-0019	Pibal Report #70-11
b. PROJECT NO.	
c.	9b. OTHER REPORT NO(S) *(Any other numbers that may be assigned this report)*
d.	

10. DISTRIBUTION STATEMENT

U. S. Army Research Office
Distribution of this document is unlimited

11. SUPPLEMENTARY NOTES	12. SPONSORING MILITARY ACTIVITY
	U.S. Army Research Office-Durham

13. ABSTRACT

Biaxial and uniaxial experiments have been conducted on a thin sheet of natural rubber, which can be assumed to be incompressible, isotropic, and perfectly elastic. The strain energy function and constitutive equations have been determined, and the material is classified as a Generalized Rivlin-Mooney type.

Biaxial experiments were then conducted on the same sheet with a circular cutout and stress concentration factors were obtained. Results indicate a significant increase in the factor with increased displacements.

A modified Particle-In-Cell (P.I.C.) method has been developed and analytical results were obtained for a sheet with a rigid circular inclusion. It is shown that the stress concentration factor for a Rivlin-Mooney material increases with increasing deformations, a result which is in qualitative agreement with solutions obtained by other methods [31,32]. The use of the Generalized Rivlin-Mooney material, however, leads to a decrease in stress concentration with increasing deformations.

DD FORM 1 NOV 65 1473

UNCLASSIFIED

Security Classification

UNCLASSIFIED
Security Classification

14. KEY WORDS	LINK A		LINK B		LINK C	
	ROLE	WT	ROLE	WT	ROLE	WT
Nonlinear Elasticity						
Stress Concentration						
Elastomeric Sheet						

Security Classification